

RESPONSE TO REVIEWERS

REVIEW 1

This paper analyzed the carbon use efficiency (CUE, the ratio of NPP to GPP) of a Mediterranean forest and its response to drought. It found the CUE is conservative compared with GPP and NPP but still decreases with drought. The data reported in this study is informative and useful to understanding plant responses to drought and modeling studies. The paper is well written overall, but I still have some concerns on the presentation and explanations of the data.

- 1. The authors also reported heterotrophic respiration (R_h), ecosystem respiration (R_{eco}) and ecosystem net production (NEP) besides GPP, NPP, and R_a that are necessary for estimating CUE. They are not related to the objectives of this study: CUE and its responses to drought. To evaluate R_h , R_{eco} , and NEP, it needs to have the data of litter and soil carbon decomposition rates that are not described in this study. R_{eco} is the sum of R_a and R_h . NEP is the difference between GPP and R_{eco} , or NPP and R_h . So, they are not independent variables. It seems not necessary to include the data of R_h , R_{eco} , and NEP in this paper.*

The starting point of this work were the contrasted highly significant linear declines of NEP, GPP and R_{eco} with drought severity evaluated through the Water Stress Integral (WSI) (see Table 1 lines 1 to 3 and Figure 1) that we observed over a continuous period of 10 years. One central objective of this work is to examine how drought affects CUE. However, we had other objectives:

1. We wish to provide a picture of the carbon fluxes and stock in our ecosystems. We believe this is important as it will facilitate future synthesis and future comparison among ecosystems. Actually, parameters NEE, GPP, and R_{eco} are widely and routinely estimated among ecosystems (through the different national, European and world networks) and thus the most robustly comparable.
2. We also wanted to evaluate the responses of NEP and R_{eco} to WSI, as it is not common to have more than a decade of these data together with WSI. We think this information is worthy and should be kept. Moreover, with these data we have

tried to close a complete ecosystem carbon balance. We have used the same equations used by other authors to this end, assuming a steady-state of ecosystem compartments: $GPP = ANPP + R_{aa} + TBCF$; $TBCF = BNPP + R_{ab} + R_h$; $R_h = R_{eco} - R_{aa} - R_{ab}$. We acknowledge some limitations to this approach coming from estimations of R_{ab} and R_h . However, we note our values are similar to those obtained by other authors (Rodeghiero and Cescatti 2006; Litton and Giardina 2008).

In our paper we used concurrent data based on shorter periods to constrain our estimates. Unfortunately it was difficult to measure continuously the soil CO_2 efflux F_{sol} such as did Misson et al. (2010) for two successive years, or leaf dark respiration or stem CO_2 efflux by daily sampling as did Rodríguez-Calcerrada et al. (2011 and 2014). All these values help us to propose a coherent estimate of the whole carbon budget. The methods concerning measurement of F_{sol} , and upscaling to the whole-canopy leaf dark respiration and stem CO_2 efflux were detailed in the referenced corresponding papers:

Misson, L., Rocheteau, A., Rambal, S., Ourcival, J.-M., Limousin, J.-M., and Rodriguez, R.: Functional changes in the control of carbon fluxes after 3 years of increased drought in a Mediterranean evergreen forest?, *Glob. Change Biol.*, 16, 2461–2475, doi:10.1111/j.1365-2486.2009.02121.x, 2010

Rodríguez-Calcerrada, J., Jaeger, C., Limousin, J. M., Ourcival, J. M., Joffre, R., and Rambal, S.: Leaf CO_2 efflux is attenuated by acclimation of respiration to heat and drought in a Mediterranean tree, *Funct. Ecol.*, 25, 983–995, doi:10.1111/j.1365-2435.2011.01862.x, 25 2011.

Rodríguez-Calcerrada, J., Martin-StPaul, N. K., Lempereur, M., Ourcival, J.-M., Rey, M.-D.-C., Joffre, R., and Rambal, S.: Stem CO_2 efflux and its contribution to ecosystem CO_2 efflux decrease with drought in a Mediterranean forest stand, *Agr. Forest Meteorol.*, doi:10.1016/j.agrformet.2014.04.012, 2014

2. *The description of data collection and analysis I can't get a clear picture on how GPP, NPP, and R_a were measured or estimated. I think the sections of 2.2, 2.5, and can be put together, because they are all about the estimation of carbon fluxes (GPP, NPP, R_a , et al.). But I still can't get how R_a is estimated. I also don't know how many samples were taken and how the uncertainty of data was estimated. There are no error bars for the data in Fig. 1 (GPP and NPP).*

We did not plot error bars in GPP and NEP (not NPP) in Figure 1. We have an error estimate did by Stauch et al. (2008) on NEE. In our eddy flux tower, she evaluated this error to be 6.5%. Further Misson et al. (2010) expected errors of 20, 30 and 40 g C m⁻² for NEE, GPP and R_{eco} , respectively (line 10 page 12). Furthermore as NEE, GPP and R_{eco} constitute direct

measurements of C fluxes at the stand scale, they are less subjected to uncertainties than the other individual fluxes based on upscaling methodologies (e.g. production, respiration).

I think the sections of 2.2, 2.5, and can be put together, because they are all about the estimation of carbon fluxes (GPP, NPP, R_a , et al.)

OK we moved 2.2

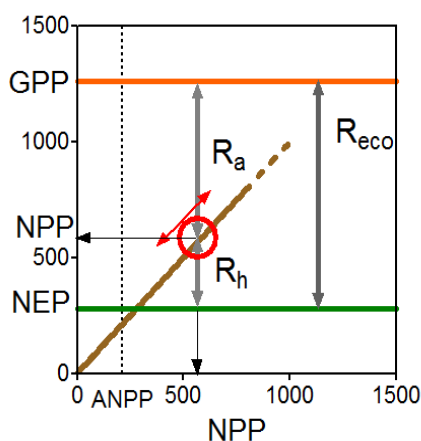


Figure 1. Scheme showing how the biometric estimate of NPP determines the partition of R_{eco} in its components R_a and R_h . In this figure, we plot GPP, NEP and NPP at their average values. We could see how error in estimating NPP propagates in R_a and R_h .

We acknowledge that we have provided few explanations of the methods we used to estimate R_a (see Figure 1). Perhaps the reviewer is confused because in the methods (page 12, lines 18-23) it seems that we used Rambal et al (2004) to estimate R_g and then R_m from R_{eco} ; but later (in page 16, lines 14-28) it appears we sum up R_{aa} and R_{ab} .

In order to make clearer the steps we have followed to obtain R_a , (R_h), R_{aa} , (R_{leaf} , R_{astem}), R_{ab} and other fluxes, and also how we have combined the different fluxes to get the CUE, we draw the following figure. In this figure (Figure 2) we separated stand scale fluxes (grey), fluxes measured punctually at the organ or soil levels and up-scaled to the stand level (brown), and punctual biomass estimates (green). We suggest putting this graph as an appendix.

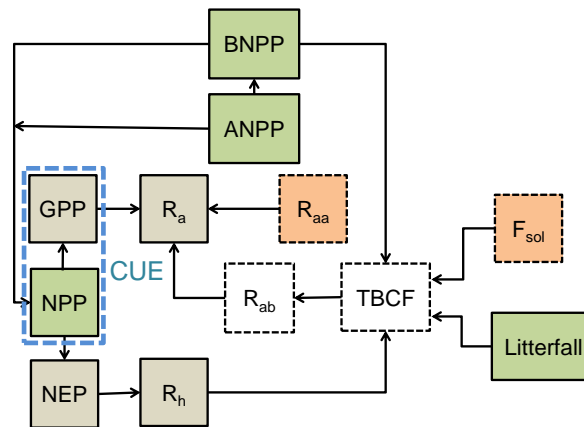


Figure 2. Method used in closing the whole-ecosystem carbon balance. Arrows are the information lines. The grey boxes surrounded by a continuous line are the ecosystem scale flux measurements yielding NEP, GPP and R_{eco} values. The green boxes are the continuous biometric measurements of the growth components. The boxes surrounded by a dashed line mean discrete measurements. The brown boxes are for discrete measurements of fluxes (leaf, stem and soil) up-scaled in time and space.

Stauch, V. J., Jarvis, A. J., & Schulz, K. (2008). Estimation of net carbon exchange using eddy covariance CO_2 flux observations and a stochastic model. *Journal of Geophysical Research: Atmospheres (1984–2012)*, 113(D3).

3. *Carry-over effect of NPP on CUE* The author used different years' GPP, NPP, and soil water stress index to show the relationship between CUE and WSI. But as the authors said "The leaf production was not related to the current year WSI but to the previous year WSI" (line 10, page 8690), the CUE is partly determined by last year's GPP and NPP. So, there are must be some carry-over effects on the estimation of CUE, which would bias the relationship between CUE and WSI. This should be discussed.

The insensitivity of $ANPP_{leaf}$ to current-year WSI alters NPP sensitivity to current-year WSI. In a wet year following a drier year, $ANPP_{leaf}$ would be lower than expected by current climate. NPP may decline, but GPP too (and CUE?). We think in a wet year following a drier one, CUE could decline because $ANPP_{stem}$ would be ruled by current climate and would be high as corresponds to a wet year, while leaves would be produced in less amount due to past-year drought carry-over effect on leaf number; the ratio of photosynthetic to non-photosynthetic tissue would decline and CUE could decline. Perhaps the strategy of holm oak to buffer the hydraulic system from climatic extremes has a penalty on CUE.

In other words, current-year drought causes GPP and less so R_a to decline, so that CUE declines slightly. If the previous year was drier, CUE could be lower than if the previous year was wet, because of the one-year-lag effect of drought on leaf production, but still, CUE will decline (slightly) due to current-year drought effects on leaf photosynthesis and less so plant respiration.

Minor concerns:

1. *Line 14, page 8681 “water stress integral (WSI)” may be just called “water stress index”.*

We do not agree. We prefer to continue using the term first proposed by Myers (1988) as water stress integral, with the same meaning.

4. *Line 17, page 8682 “LMA”. Define it before using.*

Ok we have detailed it.

5. *Lines 18_20, page 8683: “They found annual fine root production”: This sentence is confusing. It’s leaf/root or root/leaf?*

They found annual fine root production over the 0-60 cm soil layer was quasi identical to the annual leaf production and found a ratio of fine root/leaf production of 1.04. We corrected this value to consider fine roots production over the whole profile (4.5m), by considering (i) the distribution of fine roots over the soil profile proposed by Jackson et al. (1997) for sclerophyllous shrubs and trees, and (ii) the increase of fine root turnover rate with depth (López et al., 2001). We obtained a ratio of fine root/leaf production of 1.25.

6. *Lines 17_25, page 8685 and elsewhere: The authors presented the “CV” of some data. I’m just wondering what “CV” can tell the readers. I think it’s just represent “inter-annual variations” of these variables.*

Yes, it is between-year variation.

7. Line 25, page 8690: Fig. 6 should be Fig. 5

Corrected

8. Fig. 1 GPP and NEP. I'd like to see NPP in this figure.

We choose to plot first data coming from the eddy tower

9. Fig. 6 curve R_a/GPP . Since CUE (NPP/GPP) has been shown in figure 5, it's not necessary to present R_a/GPP . To me, the figure is redundant.

There exist some redundancies between both figures. We agree but we wished to maintain this figure because some literature results used R_a/GPP rather than CUE.

Fig. A2. I'd like to see a curve of LAI vs. WSI?

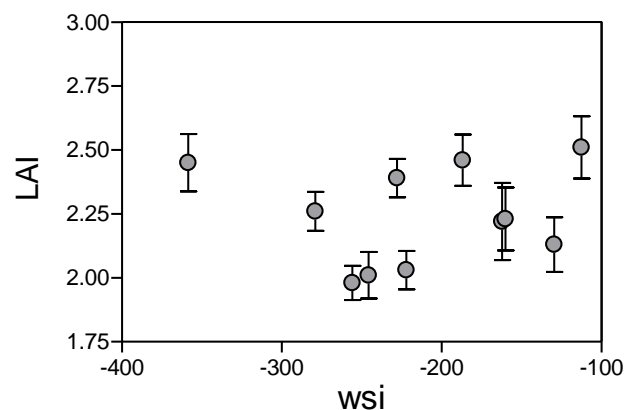


Figure 3. Relationship between WSI and LAI. This relationship is not significant.

REVIEWER 2

Thank you for the careful revision of this manuscript. A point-by-point response follows.

Carbon sequestration by forests is sensitive to drought. This paper studied the drought severity of GPP and its partitioning among carbon pools in a Quercus ilex coppice using field measurements. This is a well-written and interesting paper. It is publishable after some minor modifications.

1. *Field capacity is assigned 205 mm. Is this value measured or estimated?*

Field capacity is defined here as the water stored in the soil two to three days after a large rainfall event, when excess water drains away by the downward forces of gravity. This value of field capacity assumes that the water removed from the soil profile is only removed by gravity, not through plant transpiration or the soil evaporation. From our measurements of soil water storage (see figure 1) we fixed this value to 205 mm. Even if the fine fraction of the soil is fine-textured (clay loam), we considered it to be at field capacity when the water potential in the soil is at -33 kPa. So at a relative water content $SWS/FC = 1$, the retention curve is at a potential of -33 kPa.

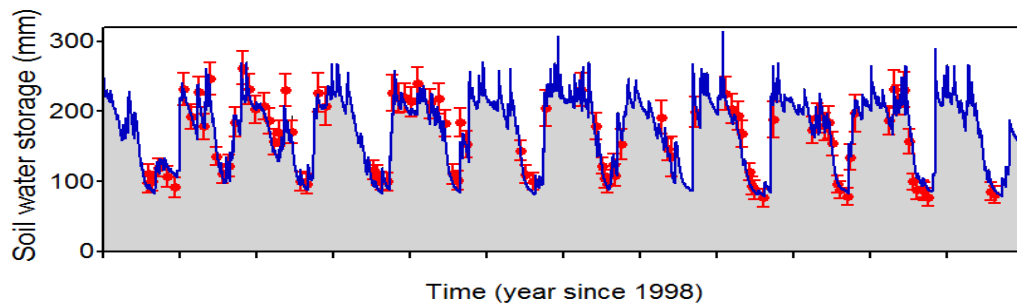


Figure 1. Time course of soil water storage. The blue line is the continuous simulated daily values (see part 2.4). Red points (+ SEM) are the discrete measurements obtained by integrating soil water content profiles. During the wet seasons or after large rainfall events we observed that the rate of change in soil water content presented a significant change at about 205 mm

2. *Some valuables, such as $BNPP_{coarse}$ and $BNPP_{fine}$, were estimated. Please analyze the uncertainties of these estimates.*

There are several methodological pitfalls associated with sampling perennial root biomass and estimating its belowground production in our *Quercus ilex* coppice, where 90% of soil volume is stones below 50 cm depth. These pitfalls include the difficulty to sample for deep roots and to extend the sampling to many replicate trees. To account for the missing root parts, we corrected our estimates of total root biomass by adding 10% of sampled root biomass. Including other data sets from colleagues in North East Spain in *Quercus ilex*, we obtained an isometric partitioning between above- and below-ground biomass (see for instance Hui et al. 2014 for a substantial account).

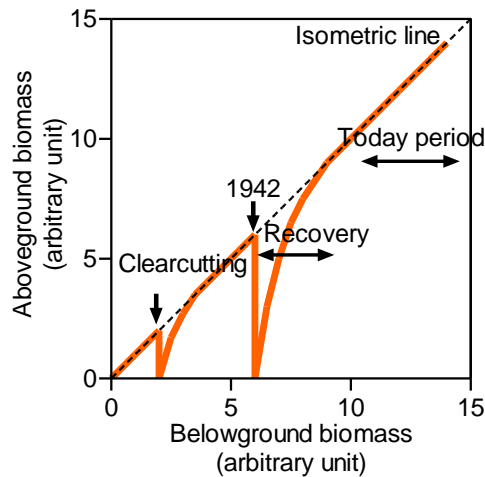


Figure 2 Theoretical scheme showing the time courses of belowground and aboveground biomass of an individual of *Quercus ilex* submitted to clearcutting. Two successive clear cuts have been represented followed by their recovery phases. For the today period we observed that both biomasses were isometrically related.

The isometric hypothesis has been disputed in several studies. Our contribution to the ongoing debate about allometry of biomass partitioning is more an empirical evidence than a theoretical advancement (see Figure A1). It will help understanding the biomass partitioning pattern in coppices, which has been largely overlooked despite its importance in ecosystem modeling and ecology. We postulate that the error we made in estimating $BNPP_{coarse}$ is equivalent to the one we made in evaluating the change in stem biomass; approximately 20% (see Figure 2).

The production and turnover of fine roots contributes significantly to carbon cycling in forest ecosystems. Unfortunately, limited observations of fine root dynamics make difficult to quantify and predict fine root growth pattern and productivity. The errors in estimating fine root biomass production originates from the fine root turnover rate and the maximum standing belowground biomass. Some compilations of global database help us to constraint and validate the estimate we used in this work. In Jackson et al. (1997) (see also Gill and Jackson, 2000) most of the results retained for describing the so-called class “sclerophyllous shrubs and trees” are from the works that Jochen Kummerow did in Mediterranean-type ecosystems in California and in Southern France, where some of the species are Mediterranean evergreen oaks. More recently, compilation of a new global database estimated fine root production and fine root turnover ranged in the boreal, temperate and tropical forests (Finér et al. 2011).

In our work we used data obtained on the same species growing in coppice under close ecological conditions. We adopted as strong hypothesis the main results of López et al., 2001. They found annual fine root production over the 0-60 cm soil layer was quasi identical to the

annual leaf production and found a ratio of fine root/leaf production of 1.04. We corrected this value to consider fine roots production over the whole profile (4.5m), by considering (i) the distribution of fine roots over the soil profile proposed by Jackson et al. (1997) for sclerophyllous shrubs and trees, and (ii) the increase of fine root turnover rate with depth (López et al., 2001). We obtained a ratio of fine root/leaf production of 1.25. We postulate that the error we made in estimating $BNPP_{fine}$ is greater to the one we made in evaluating $BNPP_{coarse}$; approximately 30% as most studies did on this component we could not reach easily.

Finér, L., Ohashi, M., Noguchi, K., & Hirano, Y. (2011). Fine root production and turnover in forest ecosystems in relation to stand and environmental characteristics. *Forest Ecology and Management*, 262(11), 2008-2023.

Gill, R. A., & Jackson, R. B. (2000). Global patterns of root turnover for terrestrial ecosystems. *New Phytologist*, 147(1), 13-31.

Hui, D., Wang, J., Shen, W., Le, X., Ganter, P., & Ren, H. (2014). Near Isometric Biomass Partitioning in Forest Ecosystems of China. *PloS one*, 9(1), e86550

Jackson, R. B., Mooney, H., and Schulze, E.-D. (1997). A global budget for fine root biomass, surface area, and nutrient contents, *P. Natl. Acad. Sci. USA*, 94, 7362–7366,

López, B., Sabaté, S., and Gracia, C. (2001). Fine-root longevity of *Quercus ilex*, *New Phytol.*, 151, 437-441.

3. *WSI was used as the indicator of drought severity. Did you try use anomaly or standard precipitations index to indicate the drought severity?*

We tested some concurrent drought severity indices. In Mediterranean-type climate areas, the yearly rain amount is the worst descriptor of drought severity (see line 7 page 13). Below we present, for two consecutive years, 2005 and 2006, the time courses of soil water storage (SWS) and predawn leaf water potential (figure 3a) simulated by our soil water model, used to calculate the water stress integral (WSI). We compared it with some other drought indices (data not shown): drought length (that is, the day at which water content expressed in percent of field capacity was below a given threshold of 0.7 or 0.4), and drought intensity (the area between the soil water storage corresponding to the retained threshold and the SWS time course). We retained WSI because the predawn water potential controls many plant functions and has been largely proved efficient in forest ecology (see discussion lines 8 to 20 on page 17). It is well adapted to the non-linear nature of the soil water retention curve (particularly on fine-textured soil) in comparison with drought length or drought intensity, for instance. We also present (Figure 3b), for comparison, the time course of the SPI₃ (standardized precipitation index with a time window of 3 months); negative values of SPI₃ mean drought

periods. We observe that the SPI_3 is able to identify well the dry months in 2006. It suggests a dry Spring in 2005 followed by a summer period without any significant drought, in opposition to our simulations and observations. Its standardized nature make difficult to use it over a rather short period of 10 years. Our calculations of SPI_3 presented in Figure 3b have been done using 30 years of monthly rainfall amounts.

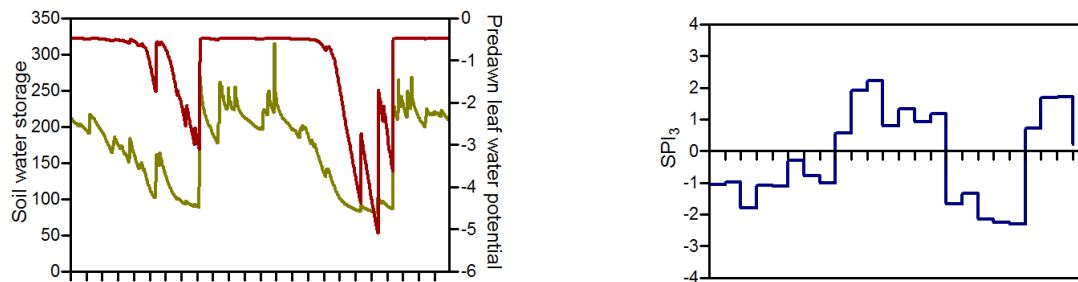


Figure 3. a) Daily time courses of soil water storage in mm (green line) and of predawn leaf water potential in MPa (red line) for two consecutive years 2005 and 2006; b) course of monthly Standardized Precipitation Index (SPI). Different SPIs are obtained for different time-scales representing the cumulative rainfall amount balance over the previous k months. Here we plotted SPI with a time window of $k=3$ months or SPI_3 . Negative values mean months with water limitation or drought and positive values are for well-watered conditions or excess water.

1 | HOW DROUGHT SEVERITY CONSTRAINS GPP AND ITS PARTITIONING
2 | AMONG CARBON POOLS IN A *QUERCUS ILEX* COPPICE?
3 |

4 | Rambal S^{1, 5}, Lempereur M^{1, 6}, Limousin JM², Martin-StPaul NK^{1, 3, 7}, Ourcival JM¹,
5 | Rodríguez-Calcerrada J⁴

6 |
7 | ¹CEFE-CNRS, UMR5175, 1919 Route de Mende, F-34293 Montpellier, Cedex 5, France

8 | ²Department of Biology, University of New Mexico, MSC03 2020, Albuquerque, New
9 | Mexico 87131-0001, USA

10 | ³Laboratoire Ecologie Systématique et Evolution CNRS, Orsay, F-91405, France

11 | ⁴Grupo de Investigación en Genética y Fisiología Forestal, E.T.S.I. Montes, Universidad
12 | Politécnica de Madrid. Ciudad Universitaria S/N. 28040 Madrid, España

13 | ⁵Universidade Federal de Lavras, Departamento de Biologia, CP 3037, CEP 37200-000,
14 | Lavras, MG, Brazil

15 | ⁶Agence de l'Environnement et de la Maîtrise de l'Energie 20, avenue du Grésillé- BP 90406
16 | 49004 Angers Cedex 01 France

17 | ~~⁶French Environment and Energy Management Agency, 20 avenue du Grésillé, BP 90406, F-~~
18 | ~~49004 Angers, Cedex 01, France~~

19 | ⁷INRA, URFM, Ecologie des Forêts Méditerranéennes, UR 629, Domaine Saint Paul, Site
20 | Agroparc, F-84914 Avignon Cedex 9, France

21 |

22 **ABSTRACT**

23 The partitioning of photosynthates toward biomass compartments has a crucial role in the
24 carbon sink function of forests. Few studies have examined how carbon is allocated toward
25 plant compartments in drought prone forests. We analyzed the fate of *GPP* in relation to
26 yearly water deficit in an old evergreen Mediterranean *Quercus ilex* coppice severely affected
27 by water limitations. ~~Gross, and net-e~~Carbon fluxes between the ecosystem and the
28 atmosphere were measured with an eddy-covariance flux tower running continuously since
29 2001. Discrete measurements of litterfall, stem growth and f_{APAR} allowed us to derive annual
30 productions of leaves, wood, flowers and acorns and an isometric relationship between stem
31 and belowground biomass has been used to estimate perennial belowground growth. By
32 combining eddy-covariance fluxes with annual productions (*NPP*), we managed to close a C
33 budget and derive values of autotrophic, ~~and~~ heterotrophic respirations, ~~NPP~~ and carbon use
34 efficiency (*CUE*, the ratio between *NPP* and *GPP*). Average values of yearly *NEP*, *GPP* and
35 *R_{eco}* were 282, 1259 and 977 g C m⁻². The corresponding *ANPP* components were 142.5, 26.4
36 and 69.6 g C m⁻² for leaves, reproductive effort (flowers and fruits) and stems. ~~Gross and~~
37 ~~net~~*NEP*, *GPP* and *R_{eco}* ~~carbon exchange between the ecosystem and the atmosphere~~ were
38 affected by annual water deficit. Partitioning to the different plant compartments was also
39 impacted by drought, with a hierarchy of responses going from the most affected, the stem
40 growth, to the least affected, the leaf production. The average *CUE* was 0.40, which is well in
41 the range for Mediterranean-type forest ecosystems. *CUE* tended to decrease more slightly in
42 response to drought than *GPP* and *NPP*, probably due to drought-acclimation of autotrophic
43 respiration. Overall, our results provide a baseline for modeling the inter-annual variations of
44 carbon fluxes and allocation in this widespread Mediterranean ecosystem and highlight the
45 value of maintaining continuous experimental measurements over the long term.

46

47 **1. INTRODUCTION**

48 Forest ecosystems exert a strong influence on the global C cycle (Bonan, 2008) as forests may
49 contribute up to 60% of the total land carbon uptake (Beer et al., 2010). Estimations and
50 simulations of carbon uptake by forest ecosystems have been greatly improved in recent
51 decades, but unfortunately how this assimilated C is transferred from the atmosphere to the
52 terrestrial biomass remains poorly known. Luo et al. (2011) highlighted a lack of mechanistic
53 understanding on this question and suggested “to develop generalizable models of C
54 allocation to biomass growth of plant parts, respiration, nonstructural C reserve, reproduction
55 and defense” as a challenging issue. A recent synthesis has demonstrated that the partitioning
56 of gross photosynthetic production (*GPP*) among above- and below-ground production and
57 respiration can vary greatly across biomes according to climate and fertility (Litton and
58 Giardina, 2008). However, a more detailed understanding of how environmental factors affect
59 the distribution of C among the different tree parts at the ecosystem scale remains a crucial
60 step to improve the accuracy of local and global vegetation models (Fatichi et al., 2013;
61 Leuzinger and Quinn Thomas, 2011).

62 Understanding C allocation patterns appears particularly important in drought prone
63 areas, such as those with a Mediterranean-type climate, which are particularly vulnerable to
64 the ongoing climate change (Giorgi, 2006). According to global and regional climate models,
65 Mediterranean-type ecosystems (MTEs) will suffer longer and more intense droughts as a
66 result of 1) increasing temperature and decreasing rainfall (Hoerling et al., 2011), 2) a change
67 in large-scale circulation conditions (Kjellström et al., 2013), and 3) the persistence of heat
68 wave anomalies (Jaeger and Seneviratne, 2011). In MTEs, drought is already the prevailing
69 constraint on the net ecosystem productivity (*NEP*) (Allard et al., 2008; Grünzweig et al.,
70 2003). This sink strength is likely modified by the differential sensitivity to water limitation of
71 leaf photosynthesis and whole-tree respiration, and of the C allocation to short- and long-lived
72 pools. The representation of C use in models currently lacks consensus and is achieved by a
73 plethora of concurrent approaches (Franklin et al., 2012). This modeling deficiency seems to
74 be due to the difficulty in interpreting this information in generic schemes that are valid under
75 a wide range of conditions, and particularly water limitation.

76 So far, studies addressing the question of C-use in MTEs have relied on the coupling
77 of field data of standing biomass and growth compartments with simulation models.
78 Pioneering works started in the 70s onwards (López et al., 2001b). Oechel and Lawrence
79 (1981) applied the process-based model MEDECS to eight woody Mediterranean species

80 growing in California chaparral and Chilean matorral. The model scaled up leaf level
81 respiration and assimilation together with stem respiration to yield yearly C budgets using a
82 radiation transfer scheme. The hierarchy of C allocation to leaves, stems, and roots followed
83 species-specific rules and a phenological calendar. From this modeling exercise, the authors
84 deduced changes in C use that deeply modified the respiratory costs in response to changes in
85 air temperature. Yet, the effect of drought on C use remains more difficult to understand and
86 simulate.

87 Forests and woodlands dominated by the evergreen oak *Quercus ilex* L. occupy large
88 areas in the surrounding of the Mediterranean Sea (Quézel and Médail, 2003) and are
89 emblematic of the MTEs. Due to its resprouting nature, *Q. ilex* can persist in the same place
90 for hundreds of years and populations display minimal changes in stool number per area. Very
91 large survival rates and fast recovery of its foliage after complete dieback (Lloret et al., 2004)
92 reflect its high ability to damp climate extremes (Misson et al., 2011). In contrast, co-
93 occurring obligate seeders are subjected to all the vicissitudes of regeneration, and are
94 particularly affected by drought mortality at the seedling stages and by wildfires (Ackerly,
95 2004; Zavala, 1999). The growing interest in resprouting ability as a major plant functional
96 trait is reflected in a number of recent contributions aimed at understanding the biogeography
97 and developing functional models of resprouting species (Clarke et al., 2010; Vesk and
98 Westoby, 2004; Vilagrosa et al., 2014). Resprouters have the particularity to store
99 considerable amounts of C belowground at the cost of high maintenance respiration (Iwasa
100 and Kubo, 1997). Characterizing the ecosystem C use for such species is important for
101 managing and predicting the response of Mediterranean forests to the on-going climate
102 changes.

103 The functioning of *Quercus ilex* stands in Southern France was simulated by Hoff et
104 al. (2002) and Hoff and Rambal (2003) using the Forest-BGC model. C-use rules in this
105 simple model are implemented so as to follow an optimal trajectory: trees use C first into
106 leaves and fine roots for maximizing productivity while minimizing water limitation; finally
107 stems appear as an end-product built with the remaining C. Other modeling exercises with *Q.*
108 *ilex* ecosystems also retained water-related constraints for their C-use rules. Gracia et al.
109 (1999) developed a dynamic growth model where the partitioning of growth between leaves
110 and perennial wood compartments is performed so as to fulfill the assumptions of the pipe
111 model theory (Shinozaki et al., 1964; see also Mäkelä, 1986 for substantial accounts;
112 Valentine, 1985), i.e. so as to maintain the sap area/foliage area ratio constant. Gracia et al.
113 (1999) also constrain growth to fine roots to follow the functional balance hypothesis

114 (Brouwer, 1962). Both abovementioned modeling exercises yielded credible results when
115 validated against yearly variations of radial growth. Fortunately, the increasing availability of
116 long term field measurements of productivity and eddy covariance fluxes can now help to
117 refine these previous modeling hypotheses.

118 In this study, our main objectives were: 1) to evaluate the fraction of *GPP* partitioned to
119 above- and below-ground parts in a *Quercus ilex* forest by comparing different ecosystems
120 across a range of climate, management, and drought resistance of dominant species, and 2) to
121 assess how year-to-year variation in drought severity impacts the partitioning of *GPP* between
122 production and respiration, and among above- and below-ground C pools. For these purposes,
123 we used long-term data of eddy covariance fluxes and primary productivity of aboveground
124 components (leaves, flowers, fruits and stems), plus punctual data of root biomass taken from
125 literature and our own excavation of four *Q. ilex* trees.

126

127 2. MATERIAL AND METHODS

128 2.1. Site description

129 The study site is located 35km north-west of Montpellier (southern France), on a flat plateau
130 in the Puéchabon State Forest (3°35'45"E, 43°44'29"N, 270m a.s.l.). This forest has been
131 managed as a coppice for centuries and the last clear cut was performed in 1942. Vegetation is
132 largely dominated by a dense overstorey of the evergreen oak *Quercus ilex*. The top canopy
133 height is about 5.5m. In 2010, stem density was 4900 stems·ha⁻¹. Stems with diameter at
134 breast height (*DBH*) < 4cm represented 6 % of total stems, whereas those with *DBH* > 10cm
135 represented 20.6 %. Understorey species *Buxus sempervirens*, *Phyllirea latifolia*, *Pistacia*
136 *terebinthus* and *Juniperus oxycedrus*, compose a sparse shrubby layer with a percent cover
137 lower than 25% and a height less than 2 m.

138 The area has a Mediterranean-type climate. Rainfall mainly occurs during autumn and
139 winter, with about 80% taking place between September and April. The mean annual
140 precipitation is 916 mm, with a range of 556-1549 mm recorded over the 1984-2011 period.
141 Mean annual temperature over the same period was 13.0°C, with a minimum in January
142 (5.5°C) and a maximum in July (22.9°C). The rocky soil is formed on Jurassic limestone; on
143 average, the volumetric fractional content of stones and rocks is about 0.75 for the top 0-50
144 cm and 0.90 below. The stone-free fine fraction of the soil is a homogeneous silty clay loam
145 (USDA texture triangle) within the top 0-50cm layer (38.8% clay, 35.2% silt and 26% sand).
146 The fine fraction fills up the space between stones and rocks and provides a source of water
147 throughout the long dry summers for the deep-rooted *Q. ilex* (Rambal, 2011). The highly
148 permeable soil prevents any surface runoff to occur even for high intensity rain events.

149

150 ~~2.2.1.1. Carbon fluxes and ancillary data~~

151 ~~Daily climate data, further used as model inputs for a water budget model, came from a~~
152 ~~weather station located 200 m away from the flux tower.~~

153 ~~Eddy covariance fluxes of CO₂, sensible heat, latent heat and momentum were~~
154 ~~measured continuously since 2001 at the top of a 12 m high tower that is approximately 6 m~~
155 ~~above the canopy. Our eddy covariance facility included a three-dimensional sonic~~
156 ~~anemometer (Solent R3, Gill Instruments, Lymington, England) and a closed path infrared gas~~
157 ~~analyser (IRGA, model LI 6262, Li-Cor Inc., Lincoln, Nebraska, USA), both sampling at a~~
158 ~~rate of 2Hz. Flux data were processed with protocols defined within the Carbo Europe~~
159 ~~network (www.carboeurope.org, Aubinet et al., 2000). Processing schemes of Fluxnet have~~

160 ~~been used for filling data gaps and partitioning NEP into GPP and ecosystem respiration R_{eco}~~
 161 ~~(Papale, 2006; Reichstein et al., 2005). The half-hourly fluxes were summed at a yearly time~~
 162 ~~steps for further analysis. Photosynthetically active radiation PAR_{top} was recorded at the top of~~
 163 ~~the flux tower. The fraction of PAR absorbed by the canopy (f_{APAR}) was derived from 14 PAR~~
 164 ~~sensors randomly set up in understorey locations and measuring PAR_{below} :~~

$$f_{APAR} = 1 - PAR_{below} / PAR_{top} \quad (1)$$

165

166 **2.3.2.2. Water limitation: Soil water balance model and drought index**

167 Soil water storage integrated over the rooting depth, that is c.a. 4.5 m (Rambal, 2011), has
 168 been measured during the vegetative periods of 1984-1986 and since July 1998 onwards, at
 169 approximately monthly intervals, using a neutron moisture gauge (see Hoff et al., 2002).
 170 Discrete measurements were interpolated at a daily time step with a soil water balance model
 171 proposed in Rambal (1993) and further used in Grote et al. (2009). The drainage curve
 172 relating deep drainage to soil water storage depends on the stone content over the whole-soil
 173 profile (Rambal, 1990). The model was driven by daily values of incoming solar radiation,
 174 minimal and maximal temperature and rain amount. Soil water storage and soil water
 175 potential were related by a Campbell-type retention curve (Campbell, 1985) whose
 176 parameters are strongly dependent on soil texture (see details in Rambal et al., 2003).
 177 Comparison of measured against simulated values of soil water storage (in mm), and predawn
 178 leaf water potential (in MPa), displayed very good agreement. Leaf water potential values
 179 came from discrete measurements performed on the study site (see Limousin et al., 2012 for a
 180 substantial account). For soil water storage, reduced major axis (RMA) regressions yielded
 181 $SWS_{sim} = \alpha_{rma} SWC_{obs} + \beta_{rma}$ with $\alpha_{rma} \pm$ standard-error (SE) = 0.94 ± 0.03 , $\beta_{rma} \pm$ SE = 6.0 ± 4.4 ,
 182 $R^2 = 0.93$, $F = 1137$, $p < 0.0001$ and $n = 91$; for the predawn potential, $\psi_{pdsim} = \alpha_{rma} \psi_{pdobs} +$
 183 β_{rma} with $\alpha_{rma} \pm$ SE = 0.93 ± 0.05 , $\beta_{RMA} \pm$ SE = -0.09 ± 0.09 , $R^2 = 0.840$, $F = 273.3$, $p < 0.0001$
 184 and $n = 54$. The continuous daily course of relative water content, RWC , was derived from
 185 SWS_{sim} divided by the soil water storage at field capacity that we chose to fix at 205 mm. This
 186 value corresponds to that observed after 2 days of free drainage in a cool wet period after a
 187 substantial rain event. For characterizing the whole-year water limitation, we calculated the
 188 water stress integral (WSI) as the yearly sum of ψ_{pdsim} . For days with $RWC \geq 1$ ψ_{pdsim} is fixed
 189 to -0.03 MPa. The WSI are expressed in MPa day.

190

191 2.4.2.3. Drought frequency analysis

192 The return periods for drought events were calculated, using a monthly 239-year precipitation
193 historical dataset (1762-2011) for Montpellier downtown. This dataset was scaled to our
194 experimental site using overlapping precipitation data from 1984 to 2011. As shown by
195 Rambal and Debussche (1995) and López-Moreno et al. (2009), the coefficient of variation
196 for precipitation is regionally conserved and was used to fit theoretical lognormal distribution
197 functions for extreme precipitation events at our site. Return periods were calculated as $1/p$,
198 where p is the probability of occurrence (Rambal and Debussche, 1995).

199 2.4. Carbon fluxes and ancillary data

200 Daily climate data, further used as model inputs for a water budget model, came from a
201 weather station located 200 m away from the flux tower.

202 Eddy covariance fluxes of CO₂, sensible heat, latent heat and momentum were
203 measured continuously since 2001 at the top of a 12 m high tower that is approximately 6 m
204 above the canopy. Our eddy covariance facility included a three-dimensional sonic
205 anemometer (Solent R3, Gill Instruments, Lymington, England) and a closed path infrared gas
206 analyser (IRGA, model LI 6262, Li-Cor Inc., Lincoln, Nebraska, USA), both sampling at a
207 rate of 21Hz. Flux data were processed with protocols defined within the Carbo-Europe
208 network (www.carboeurope.org, Aubinet et al., 2000). Processing schemes of Fluxnet have
209 been used for filling data gaps and partitioning NEP into GPP and ecosystem respiration R_{eco}
210 (Papale, 2006; Reichstein et al., 2005). The half-hourly fluxes were summed at a yearly time
211 steps for further analysis. Photosynthetically active radiation PAR_{top} was recorded at the top of
212 the flux tower. The fraction of PAR absorbed by the canopy (f_{APAR}) was derived from 14 PAR
213 sensors randomly set up in understorey locations and measuring PAR_{below}:

$$214 f_{APAR} = 1 - PAR_{below}/PAR_{top} \quad (1)$$

215 2.5. Leaf production and other growth components

216 *ANPP_{stem}* was estimated from yearly measurements of stem *DBH* and the allometric
217 relationship between stem biomass and stem *DBH*. *ANPP_{leaf}* and *ANPP_{reprod}* were derived
218 from monthly litter falls measured on 26 x 0.141 m² litter traps. *ANPP_{reprod}* comprised
219 flowers and acorns. *ANPP_{leaf}* was derived by estimating yearly changes of leaf mass at peak
220 leaf area index plus the amount of leaves lost as litter. Leaf production in year *t* occurred from
221 May to June and *M_{leaflitter}* was calculated as the sum of monthly values of leaf litter fallen from
222

223 August $t-1$ to July t . $M_{leaf\litter}$ was corrected for mass loss at abscission using the results of
224 Cherbuy et al. (2001):

$$225 \quad ANPP_{leaf} = M_{leaf}(t) - M_{leaf}(t-1) + M_{leaf\litter} = \Delta M_{leaf} + M_{leaf\litter} \quad (2)$$

226 Peak $LAI = PAI - SAI$ was estimated from continuous measurements of half-hourly
227 f_{APAR} between 11 AM and 1 PM from DOY 205 to 225. We first derived the plant area index
228 PAI by using a Beer's Law with an extinction parameter equal to $k/\sin\beta$. The parameter k was
229 set to 0.72 as in Rambal et al. (2003) and β is the solar elevation angle. The Stem Area Index
230 SAI was estimated by image processing of hemispheric photography. It was assumed constant
231 for the whole period and equal to 0.5 (Poncelet unpublished data). LAI was converted to leaf
232 mass with a canopy-averaged LMA-leaf mass per area of 215 g m^{-2} (see Rambal et al., 1996).
233 The below-canopy PAR sensor network was set up in 2001 so the leaf production for 2001
234 was not available. Even though *Q. ilex* is a strong emitter of terpenoids (Staudt et al., 2002),
235 biogenic volatile compound emissions are relatively minor C sources and they were neglected
236 here. So, the aboveground net productivity was computed as:

$$ANPP = ANPP_{leaf} + ANPP_{stem} + ANPP_{reprod} \quad (3)$$

237 In 2005 we observed a massive outburst of *Lymantria dispar*. Grazing from
238 caterpillars drastically impacted the leaves so we decided to exclude data from this year in our
239 calculations. Data for the belowground perennial components were obtained by excavating
240 four stumps at our site, and from literature values published by Canadell and Roda (1991) and
241 Djema (1995) for *Q. ilex* coppices growing in northeast Spain under similar climate
242 conditions. We compiled 19 biomass values for root crown, roots greater than 5 cm, and roots
243 ranging from 1 to 5 cm diameter. The whole perennial belowground compartment is the sum
244 of root crown and large roots. We obtained an isometric relationship between stem and
245 belowground biomass, with a slope equal to 1.068 ± 0.1235 ($s_{x,y} = 62.2$, $n=19$, $p<0.001$) (Fig.
246 A1). All these data came from excavations in very stony soils and only concerned the top 0-1
247 m layer. A significant part of the root system was not extracted because we have observed that
248 tap roots are able to uptake soil water at depths ranging between four and five meters
249 (Rambal, 2011). We thus applied a conservative correction factor of 10% to account for the
250 missing root part. Our belowground to aboveground ratio could be considered constant
251 whatever the stool size, so we propose an isometric partition of C between these two perennial
252 compartments. We postulate that the error we made in estimating $BNPP_{coarse}$ is equivalent to
253 the one we made in evaluating the change in stem biomass:

$$254 \quad ANPP_{stem} = \alpha BNPP_{coarse} \quad (4),$$

255 with *BNPP* representing belowground net primary productivity. Fine root production was
 256 taken from literature values. ~~López et al. (2001) (2001a)~~ López et al. (2001a) extensively
 257 monitored fine root productivity in a *Q. ilex* coppice. They found annual fine root production
 258 over the 0-60 cm soil layer to be quasi identical to leaf production (average ~~leaf-fine root~~ to
 259 ~~fine-root-leaf~~ production ratio over two years was 1.04). We correct this value for the whole
 260 profile using a ratio of 1.25, based on the distribution of fine roots over the soil profile
 261 proposed by Jackson et al. (1997) for sclerophyllous shrubs and trees, and the increase in fine
 262 root turnover rate with depth (López et al., 2001b):

$$BNPP = BNPP_{coarse} + BNPP_{fine} \quad (5)$$

263 Biomasses were converted to C using tissue-specific C contents whenever available; else 0.48
 264 was used as a default.

265

266 **2.6. Carbon budget estimate**

267 The different components were related to each other according to three identities considered
 268 here as yearly sums:

$$NPP = ANPP + BNPP = GPP - R_a \quad (6)$$

$$NEP = NPP - R_h = GPP - R_{eco} \quad (7)$$

$$R_{eco} = R_a + R_h \quad (8)$$

269 R_a is the autotrophic respiration, including both growth and maintenance components, with
 270 R_{aa} and R_{ab} standing for the above- and below-ground parts, respectively. R_h is the
 271 heterotrophic respiration. Uncertainty estimation of fluxes were around 20 g C m⁻² y⁻¹, 30 g C
 272 m⁻² y⁻¹ and 40 g C m⁻² y⁻¹ for NEE , GPP and R_{eco} , respectively (Misson et al., 2010; see also
 273 Stauch et al., 2008).

$$GPP = ANPP + R_{aa} + TBCF \quad (9)$$

274 Total belowground carbon allocation ($TBCF$) was defined as that carbon allocated
 275 belowground by plants to coarse and fine roots production, root respiration, and root exudates
 276 and mycorrhizae. $TBCF$ is either respired by microbes or roots (measured as soil-surface CO₂
 277 efflux) or stored in soil as organic matter in the litter layer or in living and dead roots.
 278 Growth respiration was calculated using the yield of growth processes Y (Thornley, 1970).
 279 This yield is the amount of biomass increment per unit of C substrate used in growth
 280 processes. It was expressed in g C of new biomass (g C of substrate used in the growth
 281 processes)⁻¹. For *Q. ilex* in Puéchabon, the Y parameter has been estimated to 0.8 g C
 282 appearing in new biomass per g of C substrate utilized (Rambal et al., 2004). In equations 6, 7

283 and 9, we neglect nonstructural C storage above or belowground. In the carbon budget we
284 wrote an equation in which C balance is zero independently of the water limitation, and
285 consequently the storage of nonstructural C pool remains constant (see Ryan, 2011; Sala et
286 al., 2010; Stauch et al., 2008 for the role of nonstructural carbohydrates in coping with
287 drought).

288

289 3. RESULTS

290 3.1. Environmental conditions and exceptional years

291 Over the study period (2001-2011), annual rain amounts ranged from 638.2 mm in 2007 to
292 1310 mm in 2003. The average value over this period (976.8 mm) was slightly greater than
293 the longer term mean (1984-2011, 916 mm). *WSI* ranged from -112.6 MPa day in the wettest
294 year (2004) to -358.6 MPa day in the driest year (2006). There was no relationship between
295 the annual rainfall amount and the annual *WSI* that the vegetation underwent. Lower *WSI*
296 occurred in years when the dry period began early in the spring season. In the driest year 2006
297 the rain deficit began in February, and from February to June the rainfall amount reached only
298 109.8 mm. We calculated a probability of 0.015 for the 2006 drought, corresponding to a
299 return period of 67 years. Other years with dry spring seasons in the historical series were:
300 1779, 1780, 1817, 1929, 1945 and 1995, but all these years displayed less severe droughts
301 than 2006. So, over the 2001-2011 period, we observed a very large range of water limitation
302 from well-watered conditions to severe drought. There was no significant covariation between
303 mean annual temperature and *WSI*.

304

305 3.2. C fluxes and production

306 The mean gross C input, *GPP*, was $1259 \text{ g C m}^{-2} \text{ yr}^{-1}$ and its coefficient of variation (CV) or
307 between year variation was 13.3%. For *NEP* the mean value was $281.7 \text{ g C m}^{-2} \text{ yr}^{-1}$ with a
308 larger CV of 33.5%; and for *R_{eco}* it was $977.2 \text{ g C m}^{-2} \text{ yr}^{-1}$, with a CV = 8.9%.

309 The average LAI was 2.25 ± 0.2 , which corresponds to a supported leaf mass of
310 231.7 g C m^{-2} ($n = 10$) with a coefficient of variation CV = 9% (Fig. A2.). Our calculation of
311 the leaf production yields an average value of $142.5 \text{ g C m}^{-2} \text{ yr}^{-1}$ ($n = 9$) with a large CV of
312 28.5%. The leaf production ranged from $202.8 \pm 77.1 \text{ g C m}^{-2} \text{ yr}^{-1}$ in 2006, the year after the
313 *Lymantria dispar* outburst and heavy grazing, to $69.6 \pm 58.2 \text{ g C m}^{-2} \text{ yr}^{-1}$ the following year in
314 2007. The reproductive effort, *ANPP_{reprod}*, evaluated in pooling flowers and acorns, displayed
315 the greater between-year variation, with a 42.5% CV, and a mean value of 26.4 g C m^{-2} . The
316 components of *ANPP_{reprod}* were, on average, $11.0 \text{ g C m}^{-2} \text{ yr}^{-1}$ for flowers (CV = 48.5%) and
317 $15.4 \text{ g C m}^{-2} \text{ yr}^{-1}$ for acorns which displayed the largest variation (CV = 87.8%). Summing
318 leaves plus flowers and acorns we obtained an average $169.6 \text{ g C m}^{-2} \text{ yr}^{-1}$, which accounted
319 only for 16.9% of the yearly *GPP*.

320

3.3. Relationships between production components and water limitation

Significant linear declines of GPP , NEP and R_{eco} with increasing drought severity were observed across years (Table 1; Fig. 1). Respectively 72% and 80% of the variance in GPP and NEP was explained by the WSI . The slopes of the $WSI-GPP$ and $-NEP$ lines were 1.91 ± 0.43 and 1.15 ± 0.20 , respectively, which means that we project a decline of GPP of $191 \text{ g C m}^{-2} \text{ yr}^{-1}$ and of NEP of $115 \text{ g C m}^{-2} \text{ yr}^{-1}$ for an increase in drought severity of 100 MPa day expressed in terms of WSI . The sensitivity to drought of R_{eco} was lower than for the two other components of the whole-ecosystem C budget, with a lower slope of 0.77 ± 0.32 associated with a lower explained variance, 42%.

Among the aboveground tree compartments, the most affected by drought was the stem (Fig. 2), with $dANPP_{stem}/dWSI = 0.42 \pm 0.10$ (Table 1; Fig. 2). According to the linear equation fitted between $ANPP_{stem}$ and WSI , the predicted allocation of C to the stem ranged from 120.9 g C m^{-2} for a hypothetical wet year that underwent a WSI of -100 MPa day (WSI in 2004 equaled -112.6 MPa day), to zero in a severely dry year with a WSI of -390 MPa day. Reproduction was also affected by water stress, with $dANPP_{reprod}/dWSI = 0.10 \pm 0.04$ (Fig. 3). In contrast, no significant relationship was found between WSI and $ANPP_{leaf}$. $ANPP_{leaf}$ was, however, significantly related to the WSI of the previous year, with a slope of 0.41 ± 0.15 and an explained variance of 52% (Fig. 4).

3.4. Relationship between CUE and water limitation

By combining the latter results with equations 6 to 9, a model of C use changes with drought severity can be proposed. Fig. 5 depicts the changes of GPP and NPP , and of the above and belowground compartments with WSI . CUE , the ratio of net primary production to gross primary production is also presented. For WSI declining from -100 MPa day in a wet year to -400 MPa day in a particularly dry year, NPP and CUE decline from 621.4 to $339.4 \text{ g C m}^{-2} \text{ yr}^{-1}$ and from 0.419 to 0.373 respectively.

Fig. 6 depicts the declines of R_{eco} , NEP and NPP with WSI and the corresponding changes of the ratios of autotrophic respiration to GPP (R_a/GPP) and heterotrophic respiration to whole-ecosystem respiration (R_h/R_{eco}). The R_a/GPP ratio increased from 0.581 to 0.627 for a change of WSI from -100 to -400 MPa day. For the same decline in WSI , the ratio of R_h/R_{eco} increased from 0.192 to 0.321, with R_h slightly increasing from 205.1 to $268.1 \text{ g C m}^{-2} \text{ yr}^{-1}$.

353 4. DISCUSSION

354 4.1. Carbon use efficiency in a Mediterranean coppice – management and drought- 355 adaptation constraints on carbon allocation rules

356 Carbon use efficiency (*CUE*), the ratio of net primary production (*NPP*) to gross primary
357 production (*GPP*), describes the capacity of forests to assimilate C from the atmosphere into
358 terrestrial biomass. *CUE* of forests has been assumed, by some authors, to be a constant value
359 of 0.47 ± 0.04 (Gifford, 2003; Waring et al., 1998), which supposes that tree respiration is a
360 constant fraction of *GPP*. Contrary to this assumption of constancy, substantial variations in
361 *CUE* have been reported in forest ecosystems. Medlyn and Dewar (1999) demonstrated that
362 *CUE* likely ranges between 0.31 and 0.59, and a more recent synthesis by DeLucia et al.
363 (2007) showed that the slope of the relationship between *NPP* and *GPP* (*CUE*) was 0.53,
364 ranging from 0.23 to 0.83 among forest types. *CUE* decreased with increasing age, and a
365 substantial portion of the variation among forest types was caused by the ratio of leaf mass-to-
366 total mass. For a ratio of leaf mass-to-total mass of 0.03 corresponding to our *Q. ilex* forest,
367 DeLucia et al. (2007) predicted a *CUE* of 0.38, similar to the mean of 0.40 obtained here, and
368 the same value that Oechel and Lawrence (1981) obtained for Californian and Chilean shrub
369 and tree species. With the process-based simulation model Gotilwa applied to a *Q. ilex*
370 coppice in northeastern Spain, Gracia et al. (1999) predicted a *CUE* of 0.41. In contrast,
371 Luysaert et al. (2007) derived a surprisingly high value of 0.54 from a global database for
372 their so-called “Mediterranean warm evergreen” biome (table 2).

373 The low ecosystem *CUE* observed at our site (around 0.40) could be due to the ancient
374 management of the ecosystem as a coppice. The large belowground biomass and respiratory
375 maintenance costs associated to this management system may alter C-use rules and constrain
376 *CUE* compared to more productive tall forests (Salomón et al., 2013). Furthermore, relatively
377 high R_{aa} (see below), could be associated to the role of above-ground organs in storing
378 nitrogen and nonstructural carbohydrates. One-year old leaves act as reservoirs contributing to
379 spring shoot growth (Cherbuy et al., 2001) while stumps and stems contain large amount of
380 parenchyma helping the tree to resprout after perturbations. Accurately quantifying the
381 relative importance of respiratory sources is an important step towards understanding the
382 whole C budget. Under the steady-state assumption of Eq. 9 (Raich and Nadelhoffer
383 1989)(Raich and Nadelhoffer, 1989), our values of *GPP*, *ANPP* and R_{aa} resulted in
384 $TBCF = 670 \text{ g C m}^{-2} \text{ yr}^{-1}$. R_{aa} was $460 \text{ g C m}^{-2} \text{ yr}^{-1}$, a value estimated from leaf respiration and
385 stem CO_2 efflux measurements made at our site and upscaled to the stand (Rodríguez-

386 Calcerrada et al., 2011; Rodriguez-Calcerrada et al., 2014). Applying the same *TBCF*
387 approach to the Misson et al. (2010) data of soil respiration for the wet 2004 year yielded a
388 *TBCF* of $630 \text{ g C m}^{-2} \text{ yr}^{-1}$. With our estimate of $BNPP = 270 \text{ g C m}^{-2} \text{ yr}^{-1}$, the R_{ab} ranged
389 between 360 and $400 \text{ g C m}^{-2} \text{ yr}^{-1}$. Finally, we could deduct an R_h ranging between 210 and
390 $230 \text{ g C m}^{-2} \text{ yr}^{-1}$ by summing the three respiration components to reach the whole-ecosystem
391 respiration R_{eco} . For comparison, the meta-analysis of Litton and Giardina (2008) report a
392 *TBCF* of $705 \text{ g C m}^{-2} \text{ yr}^{-1}$ and a *BNPP* of $334 \text{ g C m}^{-2} \text{ yr}^{-1}$, and Rodeghiero and Cescatti
393 (2006) measured, in a more mesic *Quercus ilex* coppice in which the soil respiration is very
394 high ($1079 \text{ g C m}^{-2} \text{ yr}^{-1}$), a *TBCF* of $564 \text{ g C m}^{-2} \text{ yr}^{-1}$ with the two belowground respiration
395 components R_{ab} and R_h being equal.

396

397 ***4.2. Sensitivity of carbon use and partitioning to between-year variation in water*** 398 ***limitation.***

399 To characterize year to year variations in drought severity we used a long-term cumulated
400 water stress index, the *WSI*. This concept likely originated in (Schulze et al., 1980a; Schulze
401 et al., 1980b) who related changes in normalized maximal assimilation rates and daily carbon
402 gain with the sum of water stress obtained by cumulating daily pre-dawn water potentials
403 from the day of the last rainfall to the day under consideration. Later, Wullschleger and
404 Hanson (2006) did the same with transpiration rates from trees growing in a throughfall
405 displacement experiment. This cumulated water-stress, called water-stress integral or *WSI* by
406 Myers (1988), has been applied to predict growth processes occurring at longer time scales
407 such as canopy development, litter fall dynamic and tree radial growth (Benson et al., 1992;
408 Raison et al., 1992a; Raison et al., 1992b). In our study we demonstrated that *WSI* was
409 significantly related to the current year reproductive effort, secondary growth and all
410 ecosystem C fluxes (see also Arneth et al., 1998), and useful in explaining how the previous
411 year drought limitation affected the leaf production in the subsequent year.

412 *GPP*, R_{eco} and *NEP* were largely impacted by water limitation. The decline of *GPP*
413 with drought has been observed in our site at different time and space scales. At a seasonal
414 time scale, Limousin et al. (2010) intensively discussed how leaf photosynthetic limitations
415 were related to predawn water potential. At a daily time scale, *GPP* estimated from eddy
416 correlation fluxes was related to predawn water potential (Rambal et al., 2003). The *ANPP*
417 components have also been shown to be impacted by drought severity, with a hierarchy of
418 responses going from the more affected, the stem, to the less affected, the leaves (Table 1).
419 The larger sensitivity of stem growth validates the hypothesis of the Forest-BGC model (Hoff

420 et al., 2002) in which trees allocate C first to leaves and fine roots, for maximizing
421 productivity while minimizing water stress, and then to stems, which appears as an end-
422 product built with remaining C. The reproductive effort also declined significantly with
423 increasing drought, although it represented a smaller C use. Acorn production, the larger
424 component of reproduction, has been shown to be influenced by water availability during the
425 fruiting process, in particular during the initial (spring) and advanced (summer) stages of the
426 maturation cycle (Pérez-Ramos et al., 2010).

427 The leaf production was not related to the current-year *WSI* but to the previous year *WSI*.
428 Limousin et al. (2012) observed that in *Q. ilex* the leaf litterfall was also positively correlated
429 with the previous year *WSI* so that more leaves were shed and replaced following wet years
430 than following dry years. This phenomenon might be explained by the cost-benefit hypothesis
431 (Chabot and Hicks, 1982; Kikuzawa, 1991): if the leaf carbon assimilation is reduced by
432 water limitation during a dry year, the leaf life span should increase for the leaf lifetime
433 carbon gain to pay back the leaf construction cost, and thus fewer new leaves need to be
434 produced to maintain the *LAI*. This results in an alternation of years with high leaf production
435 /shedding following wet years and years of opposite characteristics, as commonly observed in
436 evergreen species and in particular in *Q. ilex* (Montserrat-Marti et al., 2009; Ogaya and
437 Penuelas, 2006; Rapp, 1969). Such a mechanism may also contribute to maintain the water
438 transport capacity of *Q. ilex* under long lasting drought as proposed by Martin-StPaul et al.
439 (2013). Current-year drought causes GPP and less so NPP to decline, so that CUE declines
440 slightly. In a wet year following a drier one, CUE could decline because ANPP_{stem} would be
441 ruled by current climate and would be high as corresponds to a wet year, while leaves would
442 be produced in fewer amounts due to one-year-lag effect of drought on leaf production and
443 CUE could decline. Further researches could be necessary to quantify such carry-over effect
444 on CUE. Perhaps the strategy of *Q. ilex* to buffer the hydraulic system from climatic extremes
445 has a penalty on CUE.

446 Based on the responses to drought of the different compartments and on the
447 assumptions stated above (see Materials & Methods) we calculated the yearly *CUE* response
448 to drought (Fig. 65). *CUE* slightly decreased with drought from 0.419 at
449 *WSI* = -100 MPa day to 0.373 at *WSI* = -400 MPa day. Interestingly, *CUE* declined at a
450 slower rate than *GPP* and *NPP* in response to water deficit (Fig. 5). Maseyk et al. (2008)
451 reported a constant *CUE* of 0.4 in a *Pinus halepensis* forest growing in a semi-arid
452 Mediterranean-type climate and proposed that acclimation of maintenance respiration to dry
453 conditions could help maintaining *CUE* and productivity relatively high under such water

454 limited climate. Recent studies at our site showed that respiration rates declined exponentially
455 in both leaves and stems as tree water availability decreased through summer months
456 (Rodríguez-Calcerrada et al., 2011; Rodríguez-Calcerrada et al., 2014). Based on the
457 relationships between leaf/shoot predawn water potential and leaf/stem respiration we
458 calculated that stem and foliage CO₂ efflux declined by 4.7% and 7.1%, respectively, for an
459 increase of drought severity of $WSI = 100$ MPa day. Altogether, acclimation of leaf, stem and
460 root respiration to plant water deficit buffers *NPP* sensitivity to drought and contributes to
461 maintain *CUE* relatively constant across years of widely different rainfall and vegetation
462 stress. The ultimate reasons for such reduction in respiration rates are still unclear, but it
463 appears that reduced demand of respiratory products from growth and maintenance processes
464 may cause a down-regulation of mitochondrial activity (Atkin and Macherel, 2009).

465 Besides reductions in autotrophic respiration, changes in R_h contribute to complicate
466 our understanding of the impact of drought on the whole ecosystem C sink strength. In trees,
467 acclimation refers to strictly physiological processes; while in soils changes in R_h refer to
468 ecosystem-level phenomenon potentially driven by multiple mechanisms including substrate
469 depletion, changing microbial community composition, and physiological changes.
470 Substantial questions remain about its response to soil water status, the interactions with
471 substrate quality, and the role of the top soil drying-rewetting cycles (Wei et al., 2010). The
472 course of soil water content at time scales shorter than the season is not necessarily correlated
473 to the *WSI*. In Mediterranean-type ecosystems, R_h is likely more influenced by an
474 unpredictable supply of substrate to the rhizosphere than by changes in the microbial
475 community or its efficiency (Curiel Yuste et al., 2014). Finally we suggest as Hopkins et al.
476 (2013) did that substrate availability *sensu lato*, including *GPP* and storage of nonstructural C
477 pool (neglected here), may be the ultimate driver of the two respiration fluxes.

478

479 **5. CONCLUSIONS**

480 Comparative measures of ecosystem fluxes and production components across 11 years of
481 contrasting water limitations in a *Q. ilex* stand help to better understand how Mediterranean-
482 type forest ecosystems will respond to the ongoing climate change and to better project future
483 C sequestration capacity.

484 We observed a clear effect of water availability in limiting all the ecosystem fluxes
485 *GPP*, R_{eco} and *NEP*, and that the drought-induced decline in R_{eco} dampens the decline of the
486 ecosystem C sequestration under drought conditions. In parallel, all the growth components

487 were found to be affected by water limitation, with a partition of *GPP* into tissues that tends
488 to minimize the negative impacts of drought on growth. An important result is that all the
489 changes followed the same trajectory as water stress varied over a large range of conditions,
490 from a wet year to a dry year occurring only once every 67 years. We did not observe any
491 tipping point or discontinuity in the C partitioning pattern. On average, only 40% of the
492 carbon assimilated as gross photosynthesis was used to construct new tissues, with the
493 remaining 60% being respired back to the atmosphere as autotrophic respiration. This low
494 ecosystem *CUE* could be inherited from the ancient management of the ecosystem as a
495 coppice and its large amount of standing belowground biomass.

496 There are several ecological issues that question the values of the estimated C fluxes
497 and their changes with increasing drought severity. It appeared in our case that autotrophic
498 respiration by trees and heterotrophic respiration by soil microorganisms are primarily
499 responsible for mediating the larger part of the carbon exchanges between the biosphere and
500 atmosphere. Climate changes and projected increasing dryness have the potential to influence
501 the activity of trees regulating exchanges among the carbon pools. Functional ‘down-
502 regulation’ or acclimation of plant respiration could reduce the respiratory autotrophic loss of
503 ecosystems, but unlike plant components, the existence of this phenomenon in heterotrophic
504 respiration remains more controversial (Harmon et al., 2011; Wieder et al., 2013). Current
505 models can simulate *GPP* relationships with autotrophic fluxes in a warmer environment
506 (Piao et al., 2010; Wythers et al., 2013), yet the parameterization of models able to capture the
507 apparent respiratory acclimation of both R_a and R_h to water limitation of ecosystems is an
508 emerging challenge for the modeling and flux research communities. We suggest that both
509 communities should adopt a bottom-up approach to advance our understanding at tissue, tree
510 and ecosystem scales to increasingly larger time and space scales.

511

512 *Acknowledgements.*

513 A doctoral research grant was provided by the French Environment and Energy Management
514 Agency (ADEME) to ML. Projects MIND (EVK2-CT-2002-000158), DROUGHT+ (ANR-
515 06-VULN-003-01) and CARBO-Extreme (FP7-ENV-2008-1-226701) contributed in partly
516 funding this research. The authors declare no conflict of interest in relation with this work.

517

518 **REFERENCES**

- 519 Ackerly, D.: Functional strategies of chaparral shrubs in relation to seasonal water deficit and
520 disturbance, *Ecological Monographs*, 74, 25-44, 2004.
- 521 Allard, V., Ourcival, J. M., Rambal, S., Joffre, R., and Rocheteau, A.: Seasonal and annual
522 variation of carbon exchange in an evergreen Mediterranean forest in southern France, *Glob.*
523 *Change Biol.*, 14, 714-725, 10.1111/j.1365-2486.2008.01539.x, 2008.
- 524 Arneeth, A., Kelliher, F., McSeveny, T., and Byers, J.: Net ecosystem productivity, net primary
525 productivity and ecosystem carbon sequestration in a *Pinus radiata* plantation subject to soil
526 water deficit, *Tree Physiol.*, 18, 785-793, 1998.
- 527 Atkin, O. K., and Macherel, D.: The crucial role of plant mitochondria in orchestrating
528 drought tolerance, *Annals of Botany*, 103, 581-597, 2009.
- 529 Aubinet, M., Grelle, A., Ibrom, A., Rannik, U., Noncrieff, J., Foken, T., Kowalski, A. S.,
530 Martin, P. H., Berbigier, P., Bernhofer, C., Clement, R., Elbers, J., Granier, A., Grunwald, T.,
531 Morgenstern, K., Pilegaard, K., Rebmann, C., Snijders, W., Valentini, R., and Vesala, T.:
532 Estimates of the annual net carbon and water exchange of forests: The EUROFLUX
533 methodology, *Adv. Ecol. Res.*, 30, 113-175, 2000.
- 534 Beer, C., Reichstein, M., Tomelleri, E., Ciais, P., Jung, M., Carvalhais, N., Rödenbeck, C.,
535 Arain, M. A., Baldocchi, D., Bonan, G. B., Bondeau, A., Cescatti, A., Lasslop, G., Lindroth,
536 A., Lomas, M., Luyssaert, S., Margolis, H., Oleson, K. W., Rouspard, O., Veenendaal, E.,
537 Viovy, N., Williams, C., Woodward, F. I., and Papale, D.: Terrestrial gross carbon dioxide
538 uptake: Global distribution and covariation with climate, *Science*, 329, 834-838,
539 10.1126/science.1184984, 2010.
- 540 Benson, M., Myers, B., and Raison, R.: Dynamics of stem growth of *Pinus radiata* as affected
541 by water and nitrogen supply, *Forest ecology and management*, 52, 117-137, 1992.
- 542 Bonan, G. B.: Forests and climate change: forcings, feedbacks, and the climate benefits of
543 forests, *science*, 320, 1444-1449, 2008.
- 544 Brouwer, R.: Distribution of dry matter in the plant, *Neth. J. Agric. Sci.*, 10, 361-376, 1962.
- 545 Campbell, G. S.: *Soil physics with basic: Transport models for soil-plant systems*, Elsevier,
546 1985.
- 547 Canadell, J., and Roda, F.: Root biomass of *Quercus ilex* in a montane Mediterranean forest,
548 *Canadian Journal of Forest Research*, 21, 1771-1778, 1991.
- 549 Chabot, B. F., and Hicks, D. J.: The ecology of leaf life spans, *Annual Review of Ecology and*
550 *Systematics*, 13, 229-259, 1982.
- 551 Cherbuy, B., Joffre, R., Gillon, D., and Rambal, S.: Internal remobilization of carbohydrates,
552 lipids, nitrogen and phosphorus in the Mediterranean evergreen oak *Quercus ilex*, *Tree*
553 *Physiol.*, 21, 9-17, 2001.
- 554 Clarke, P. J., Lawes, M. J., and Midgley, J. J.: Resprouting as a key functional trait in woody
555 plants—challenges to developing new organizing principles, *New Phytol.*, 188, 651-654, 2010.
- 556 Curiel Yuste, J., Fernandez-Gonzalez, A., Fernandez-Lopez, M., Ogaya, R., Penuelas, J.,
557 Sardans, J., and Lloret, F.: Strong functional stability of soil microbial communities under
558 semiarid Mediterranean conditions and subjected to long-term shifts in baseline precipitation,
559 *Soil Biology and Biochemistry*, 69, 223-233, 2014.
- 560 DeLucia, E. H., Drake, J. E., Thomas, R. B., and Gonzalez-Meler, M.: Forest carbon use
561 efficiency: is respiration a constant fraction of gross primary production?, *Glob. Change Biol.*,
562 13, 1157-1167, 10.1111/j.1365-2486.2007.01365.x, 2007.
- 563 Djema, A.: Cuantificación de la biomasa y mineralomasa subterránea de un bosque de
564 *Quercus ilex L.*, MSc thesis, Instituto Agronómico Mediterráneo, Zaragoza, España, 78 p. pp.,
565 1995.

566 Fatichi, S., Leuzinger, S., and Körner, C.: Moving beyond photosynthesis: from carbon source
567 to sink-driven vegetation modeling, *New Phytol.*, 2013.

568 Franklin, O., Johansson, J., Dewar, R. C., Dieckmann, U., McMurtrie, R. E., Brännström, Å.,
569 and Dybzinski, R.: Modeling carbon allocation in trees: a search for principles, *Tree Physiol.*,
570 32, 648-666, 2012.

571 Gifford, R. M.: Plant respiration in productivity models: conceptualisation, representation and
572 issues for global terrestrial carbon-cycle research, *Functional Plant Biology*, 30, 171-186,
573 2003.

574 Giorgi, F.: Climate change hot-spots, *Geophysical Research Letters*, 33, 2006.

575 Gracia, C. A., Tello, E., Sabaté, S., and Bellot, J.: GOTILWA: An integrated model of water
576 dynamics and forest growth, in: *Ecology of Mediterranean evergreen oak forests*, Springer,
577 163-179, 1999.

578 Grote, R., Lavoie, A.-V., Rambal, S., Staudt, M., Zimmer, I., and Schnitzler, J.-P.: Modelling
579 the drought impact on monoterpene fluxes from an evergreen Mediterranean forest canopy,
580 *Oecologia*, 160, 213-223, 2009.

581 Grünzweig, J., Lin, T., Rotenberg, E., Schwartz, A., and Yakir, D.: Carbon sequestration in
582 arid-land forest, *Glob. Change Biol.*, 9, 791-799, 2003.

583 Harmon, M. E., Bond-Lamberty, B., Tang, J., and Vargas, R.: Heterotrophic respiration in
584 disturbed forests: A review with examples from North America, *Journal of Geophysical
585 Research: Biogeosciences* (2005–2012), 116, 2011.

586 Hoerling, M., Eischeid, J., Perlwitz, J., Quan, X., Zhang, T., and Pegion, P.: On the increased
587 frequency of Mediterranean drought, *Journal of Climate*, 25, 2146-2161, 10.1175/JCLI-D-11-
588 00296.1, 2011.

589 Hoff, C., Rambal, S., and Joffre, R.: Simulating carbon and water flows and growth in a
590 Mediterranean evergreen *Quercus ilex* coppice using the FOREST-BGC model, *Forest
591 Ecology and Management*, 164, 121-136, 10.1016/s0378-1127(01)00605-3, 2002.

592 Hoff, C., and Rambal, S.: An examination of the interaction between climate, soil and leaf
593 area index in a *Quercus ilex* ecosystem, *Ann. For. Sci.*, 60, 153-161, 2003.

594 Hopkins, F., Gonzalez-Meler, M. A., Flower, C. E., Lynch, D. J., Czimczik, C., Tang, J., and
595 Subke, J. A.: Ecosystem-level controls on root-rhizosphere respiration, *New Phytol.*, 199,
596 339-351, 2013.

597 Iwasa, Y., and Kubo, T.: Optimal size of storage for recovery after unpredictable
598 disturbances, *Evolutionary ecology*, 11, 41-65, 1997.

599 Jackson, R. B., Mooney, H., and Schulze, E.-D.: A global budget for fine root biomass,
600 surface area, and nutrient contents, *Proceedings of the National Academy of Sciences*, 94,
601 7362-7366, 1997.

602 Jaeger, E. B., and Seneviratne, S. I.: Impact of soil moisture–atmosphere coupling on
603 European climate extremes and trends in a regional climate model, *Climate Dynamics*, 36,
604 1919-1939, 10.1007/s00382-010-0780-8, 2011.

605 Kikuzawa, K.: A cost-benefit analysis of leaf habit and leaf longevity of trees and their
606 geographical pattern, *American Naturalist*, 138, 1250-1263, 1991.

607 Kjellström, E., Thejll, P., Rummukainen, M., Christensen, J. H., Boberg, F., Christensen, O.
608 B., and Maule, C. F.: Emerging regional climate change signals for Europe under varying
609 large-scale circulation conditions, *Climate Research*, 56, 103-119, 2013.

610 Leuzinger, S., and Quinn Thomas, R.: How do we improve Earth system models? Integrating
611 Earth system models, ecosystem models, experiments and long-term data, *New Phytol.*, 191,
612 15-18, 2011.

613 Limousin, J.-M., Longepierre, D., Huc, R., and Rambal, S.: Change in hydraulic traits of
614 Mediterranean *Quercus ilex* subjected to long-term throughfall exclusion, *Tree Physiol.*, 30,
615 1026-1036, 10.1093/treephys/tpq062, 2010.

616 Limousin, J. M., Rambal, S., Ourcival, J. M., Rodriguez-Calcerrada, J., Perez-Ramos, I. M.,
617 Rodriguez-Cortina, R., Misson, L., and Joffre, R.: Morphological and phenological shoot
618 plasticity in a Mediterranean evergreen oak facing long-term increased drought, *Oecologia*,
619 169, 565-577, 10.1007/s00442-011-2221-8, 2012.

620 Litton, C., and Giardina, C.: Below-ground carbon flux and partitioning: Global patterns and
621 response to temperature, *Functional Ecology*, 22, 941-954, 2008.

622 Lloret, F., Siscart, D., and Dalmases, C.: Canopy recovery after drought dieback in holm-oak
623 Mediterranean forests of Catalonia (NE Spain), *Glob. Change Biol.*, 10, 2092-2099, 2004.

624 López-Moreno, J. I., Vicente-Serrano, S. M., Gimeno, L., and Nieto, R.: Stability of the
625 seasonal distribution of precipitation in the Mediterranean region: Observations since 1950
626 and projections for the 21st century, *Geophysical Research Letters*, 36, L10703,
627 10.1029/2009GL037956, 2009.

628 López, B., Sabaté, S., and Gracia, C.: Annual and seasonal changes in fine root biomass of a
629 *Quercus ilex* L. forest, *Plant and Soil*, 230, 125-134, 2001a.

630 López, B., Sabaté, S., and Gracia, C. A.: Vertical distribution of fine root density, length
631 density, area index and mean diameter in a *Quercus ilex* forest, *Tree Physiol.*, 21, 555-560,
632 10.1093/treephys/21.8.555, 2001b.

633 Luo, Y., Melillo, J., Niu, S., Beier, C., Clark, J. S., Classen, A. T., Davidson, E., Dukes, J. S.,
634 Evans, R. D., Field, C. B., Czimczik, C. I., Keller, M., Kimball, B. A., Kueppers, L. M.,
635 Norby, R. J., Pelini, S. L., Pendall, E., Rastetter, E., Six, J., Smith, M., Tjoelker, M. G., and
636 Torn, M. S.: Coordinated approaches to quantify long-term ecosystem dynamics in response
637 to global change, *Glob. Change Biol.*, 17, 843-854, 10.1111/j.1365-2486.2010.02265.x, 2011.

638 Luyssaert, S., Inglima, I., Jung, M., Richardson, A. D., Reichstein, M., Papale, D., Piao, S. L.,
639 Schulze, E. D., Wingate, L., Matteucci, G., Aragao, L., Aubinet, M., Beer, C., Bernhofer, C.,
640 Black, K. G., Bonal, D., Bonnefond, J. M., Chambers, J., Ciais, P., Cook, B., Davis, K. J.,
641 Dolman, A. J., Gielen, B., Goulden, M., Grace, J., Granier, A., Grelle, A., Griffis, T.,
642 GrÜNwald, T., Guidolotti, G., Hanson, P. J., Harding, R., Hollinger, D. Y., Hutyrá, L. R.,
643 Kolari, P., Kruijt, B., Kutsch, W., Lagergren, F., Laurila, T., Law, B. E., Le Maire, G.,
644 Lindroth, A., Loustau, D., Malhi, Y., Mateus, J., Migliavacca, M., Misson, L., Montagnani,
645 L., Moncrieff, J., Moors, E., Munger, J. W., Nikinmaa, E., Ollinger, S. V., Pita, G., Rebmann,
646 C., Rouspard, O., Saigusa, N., Sanz, M. J., Seufert, G., Sierra, C., Smith, M. L., Tang, J.,
647 Valentini, R., Vesala, T., and Janssens, I. A.: CO₂ balance of boreal, temperate, and tropical
648 forests derived from a global database, *Glob. Change Biol.*, 13, 2509-2537, 10.1111/j.1365-
649 2486.2007.01439.x, 2007.

650 Mäkelä, A.: Implications of the pipe model theory on dry matter partitioning and height
651 growth in trees, *Journal of Theoretical Biology*, 123, 103-120, 1986.

652 Martin-StPaul, N. K., Limousin, J. M., Vogt-Schilb, H., Rodríguez-Calcerrada, J., Rambal, S.,
653 Longepierre, D., and Misson, L.: The temporal response to drought in a Mediterranean
654 evergreen tree: comparing a regional precipitation gradient and a throughfall exclusion
655 experiment, *Glob. Change Biol.*, 19, 2413-2426, 2013.

656 Maseyk, K., GRÜNZEIG, J. M., Rotenberg, E., and Yakir, D.: Respiration acclimation
657 contributes to high carbon-use efficiency in a seasonally dry pine forest, *Glob. Change Biol.*,
658 14, 1553-1567, 2008.

659 Medlyn, B., and Dewar, R.: Comment on the article by RH Waring, JJ Landsberg and M.
660 Williams relating net primary production to gross primary production, *Tree Physiol.*, 19, 137-
661 138, 1999.

662 Misson, L., Rocheteau, A., Rambal, S., Ourcival, J.-M., Limousin, J.-M., and Rodriguez, R.:
663 Functional changes in the control of carbon fluxes after 3 years of increased drought in a
664 Mediterranean evergreen forest?, *Glob. Change Biol.*, 16, 2461-2475, 10.1111/j.1365-
665 2486.2009.02121.x, 2010.

666 Misson, L., Degueldre, D., Collin, C., Rodriguez, R., Rocheteau, A., Ourcival, J.-M., and
667 Rambal, S.: Phenological responses to extreme droughts in a Mediterranean forest, *Glob.*
668 *Change Biol.*, 17, 1036-1048, 10.1111/j.1365-2486.2010.02348.x, 2011.

669 Montserrat-Marti, G., Camarero, J. J., Palacio, S., Perez-Rontome, C., Milla, R., Albuixech,
670 J., and Maestro, M.: Summer-drought constrains the phenology and growth of two coexisting
671 Mediterranean oaks with contrasting leaf habit: implications for their persistence and
672 reproduction, *Trees-Structure and Function*, 23, 787-799, 10.1007/s00468-009-0320-5, 2009.

673 Myers, B. J.: Water stress integral—a link between short-term stress and long-term growth,
674 *Tree Physiol.*, 4, 315-323, 1988.

675 Oechel, W., and Lawrence, W.: Carbon allocation and utilization, in: *Resource Use by*
676 *Chaparral and Matorral*, edited by: Miller, P. C., *Ecological Studies*, Springer New York, 185-
677 235, 1981.

678 Ogaya, R., and Penuelas, J.: Contrasting foliar responses to drought in *Quercus ilex* and
679 *Phillyrea latifolia*, *Biologia Plantarum*, 50, 373-382, 2006.

680 Papale, D.: Towards a standardized processing of Net Ecosystem Exchange measured with
681 eddy covariance technique: algorithms and uncertainty estimation, 3, 571-583, 2006.

682 Pérez-Ramos, I. M., Ourcival, J. M., Limousin, J. M., and Rambal, S.: Mast seeding under
683 increasing drought: results from a long-term data set and from a rainfall exclusion experiment,
684 *Ecology*, 91, 3057-3068, 10.1890/09-2313.1, 2010.

685 Piao, S., Luysaert, S., Ciais, P., Janssens, I. A., Chen, A., Cao, C., Fang, J., Friedlingstein, P.,
686 Luo, Y., and Wang, S.: Forest annual carbon cost: a global-scale analysis of autotrophic
687 respiration, *Ecology*, 91, 652-661, 2010.

688 Quézel, P., and Médail, F.: *Ecologie et biogéographie des forêts du bassin méditerranéen*,
689 Elsevier, Paris, France, 571 p. pp., 2003.

690 Raich, J., and Nadelhoffer, K.: Belowground carbon allocation in forest ecosystems: global
691 trends, *Ecology*, 70, 1346-1354, 1989.

692 Raison, R., Khanna, P., Benson, M., Myers, B., McMurtrie, R., and Lang, A.: Dynamics of
693 *Pinus radiata* foliage in relation to water and nitrogen stress: II. Needle loss and temporal
694 changes in total foliage mass, *Forest ecology and management*, 52, 159-178, 1992a.

695 Raison, R., Myers, B., and Benson, M.: Dynamics of *Pinus radiata* foliage in relation to water
696 and nitrogen stress: I. Needle production and properties, *Forest Ecology and Management*, 52,
697 139-158, 1992b.

698 Rambal, S.: *Les transferts d'eau dans le système sol-plante en région méditerranéenne*
699 *karstique: une approche hiérarchique*, Paris 11, 1990.

700 Rambal, S.: The differential role of mechanisms for drought resistance in a Mediterranean
701 evergreen shrub: a simulation approach, *Plant, Cell & Environment*, 16, 35-44, 1993.

702 Rambal, S., and Debussche, G.: Water balance of Mediterranean ecosystems under a changing
703 climate, in: *Global change and Mediterranean-type ecosystems*, Springer, 386-407, 1995.

704 Rambal, S., Damesin, C., Joffre, R., Méthy, M., and Seen, D. L.: Optimization of carbon gain
705 in canopies of Mediterranean evergreen oaks, *Annales des sciences forestières*, 1996, 547-
706 560,

707 Rambal, S., Ourcival, J. M., Joffre, R., Mouillot, F., Nouvellon, Y., Reichstein, M., and
708 Rocheteau, A.: Drought controls over conductance and assimilation of a Mediterranean
709 evergreen ecosystem: scaling from leaf to canopy, *Glob. Change Biol.*, 9, 1813-1824, 2003.

710 Rambal, S., Joffre, R., Ourcival, J., Cavender-Bares, J., and Rocheteau, A.: The growth
711 respiration component in eddy CO₂ flux from a *Quercus ilex* mediterranean forest, *Glob.*
712 *Change Biol.*, 10, 1460-1469, 2004.

713 Rambal, S.: Le paradoxe hydrologique des écosystèmes méditerranéens, *Annales de la*
714 *Société d'Horticulture et d'Histoire Naturelle de l'Hérault*, 61-67, 2011.

715 Rapp, M.: Production de litière et apport au sol d'éléments minéraux dans deux écosystèmes
716 méditerranéens: la forêt de *Quercus ilex* L. et la garrigue de *Quercus coccifera* L., Oecol.
717 Plant., 4, 377-410, 1969.

718 Reichstein, M., Falge, E., Baldocchi, D., Papale, D., Aubinet, M., Berbigier, P., Bernhofer, C.,
719 Buchmann, N., Gilmanov, T., and Granier, A.: On the separation of net ecosystem exchange
720 into assimilation and ecosystem respiration: review and improved algorithm, Glob. Change
721 Biol., 11, 1424-1439, 2005.

722 Rodeghiero, M., and Cescatti, A.: Indirect partitioning of soil respiration in a series of
723 evergreen forest ecosystems, Plant and soil, 284, 7-22, 2006.

724 Rodriguez-Calcerrada, J., Martin-StPaul, N. K., Lempereur, M., Ourcival, J.-M., Rey, M.-d.-
725 C., Joffre, R., and Rambal, S.: Stem CO₂ efflux and its contribution to ecosystem CO₂ efflux
726 decrease with drought in a Mediterranean forest stand, Agric. For. Meteorol.,
727 <http://dx.doi.org/10.1016/j.agrformet.2014.04.012>, 2014.

728 Rodríguez-Calcerrada, J., Jaeger, C., Limousin, J. M., Ourcival, J. M., Joffre, R., and Rambal,
729 S.: Leaf CO₂ efflux is attenuated by acclimation of respiration to heat and drought in a
730 Mediterranean tree, Functional Ecology, 25, 983-995, 10.1111/j.1365-2435.2011.01862.x,
731 2011.

732 Ryan, M. G.: Tree responses to drought, Tree Physiol., 31, 237-239, 2011.

733 Sala, A., Piper, F., and Hoch, G.: Physiological mechanisms of drought-induced tree mortality
734 are far from being resolved, New Phytol., 186, 274-281, 2010.

735 Salomón, R., Valbuena-Carabaña, M., Gil, L., and González-Doncel, I.: Clonal structure
736 influences stem growth in *Quercus pyrenaica* Willd. coppices: Bigger is less vigorous, Forest
737 Ecology and Management, 296, 108-118, 2013.

738 Schulze, E. D., Hall, A. E., Lange, O. L., Evenari, M., Kappen, L., and Buschbom, U.: Long-
739 term effects of drought on wild and cultivated plants in the Negev desert. I Maximal rates of
740 net photosynthesis., Oecologia, 45, 11-18, 10.1007/BF00346700, 1980a.

741 Schulze, E. D., Lange, O. L., Evenari, M., Kappen, L., and Buschbom, U.: Long-term effects
742 of drought on wild and cultivated plants in the Negev deser. II Diurnal patterns of net
743 photosynthesis and daily carbon gain, Oecologia, 45, 19-25, 10.1007/BF00346701, 1980b.

744 Shinozaki, K., Yoda, K., Hozumi, K., and Kira, T.: A quantitative analysis of plant form;the
745 pipe model theory,1, Japanese Journal of Ecology, 14, 97-105, 1964.

746 Stauch, V. J., Jarvis, A. J., and Schulz, K.: Estimation of net carbon exchange using eddy
747 covariance CO₂ flux observations and a stochastic model, Journal of Geophysical Research:
748 Atmospheres, 113, D03101, 10.1029/2007JD008603, 2008.

749 Staudt, M., Rambal, S., Joffre, R., and Kesselmeier, J.: Impact of drought on seasonal
750 monoterpene emissions from *Quercus ilex* in southern France, Journal of Geophysical
751 Research: Atmospheres (1984–2012), 107, ACH 15-11-ACH 15-19, 2002.

752 Thornley, J.: Respiration, growth and maintenance in plants, 1970.

753 Valentine, H. T.: Tree-growth models: derivations employing the pipe-model theory, Journal
754 of theoretical biology, 117, 579-585, 1985.

755 Vesk, P. A., and Westoby, M.: Sprouting ability across diverse disturbances and vegetation
756 types worldwide, Journal of Ecology, 92, 310-320, 2004.

757 Vilagrosa, A., Hernández, E. I., Luis, V. C., Cochard, H., and Pausas, J. G.: Physiological
758 differences explain the co-existence of different regeneration strategies in Mediterranean
759 ecosystems, New Phytol., 201, 1277-1288, 10.1111/nph.12584, 2014.

760 Waring, R. H., Landsberg, J. J., and Williams, M.: Net primary production of forests: a
761 constant fraction of gross primary production?, Tree Physiol., 18, 129-134,
762 10.1093/treephys/18.2.129, 1998.

763 Wei, W., Weile, C., and Shaopeng, W.: Forest soil respiration and its heterotrophic and
764 autotrophic components: Global patterns and responses to temperature and precipitation, *Soil*
765 *Biology and Biochemistry*, 42, 1236-1244, 2010.

766 Wieder, W. R., Bonan, G. B., and Allison, S. D.: Global soil carbon projections are improved
767 by modelling microbial processes, *Nature Climate Change*, 3, 909-912, 2013.

768 Wullschleger, S. D., and Hanson, P. J.: Sensitivity of canopy transpiration to altered
769 precipitation in an upland oak forest: evidence from a long-term field manipulation study,
770 *Glob. Change Biol.*, 12, 97-109, 10.1111/j.1365-2486.2005.001082.x, 2006.

771 Wythers, K. R., Reich, P. B., and Bradford, J. B.: Incorporating temperature-sensitive Q10
772 and foliar respiration acclimation algorithms modifies modeled ecosystem responses to global
773 change, *Journal of Geophysical Research: Biogeosciences*, 118, 77-90, 2013.

774 Zavala, M.: A model of stand dynamics for holm oak-aleppo pine forests, in: *Ecology of*
775 *Mediterranean Evergreen Oak Forests*, edited by: Rodà, F., Retana, J., Gracia, C., and Bellot,
776 J., *Ecological Studies*, Springer Berlin Heidelberg, 105-117, 1999.

777

778 **TABLES**

779

780 **Table 1.** Parameters of the linear ordinary least-square regression lines between the water
781 stress integral *WSI* in MPa day and components of the ecosystem yearly C budget and
782 aboveground components of the productivity. α_{OLS} is the slope of the Y vs. X relationship.
783 *GPP*, *R_{eco}* and *NEP* are gross primary productivity, ecosystem respiration and net ecosystem
784 productivity respectively, in g C m⁻² yr⁻¹. The components of the aboveground productivity
785 for leaves, reproductive effort and stem *ANPP_{leaf}*, *ANPP_{reprod}* and *ANPP_{stem}* are also expressed
786 in g C m⁻² yr⁻¹

787

Y versus X	$\alpha_{OLS} \pm SE$	$\beta_{OLS} \pm SE$	r^2	F	p	n
GPP versus WSI	1.91 ± 0.43	1675 ± 97.5	0.72	20.1	0.0021***	10
R _{eco} versus WSI	0.77±0.32	1144±72.5	0.42	5.8	0.042*	10
NEP versus WSI	1.15 ± 0.20	531.3 ± 46.2	0.80	32.2	0.0005***	10
ANPP _{leaf} (t) ^o versus WSI(t-1)	0.41 ± 0.15	233.0 ± 34.6	0.52	7.5	0.03*	9
ANPP _{leaf} (t) ^o versus WSI(t)	-0.12 ± 0.19	116.1 ± 43.6	0.05	0.41	0.54ns	9
ANPP _{reprod} versus WSI	0.10 ± 0.04	49.1 ± 8.8	0.48	7.2	0.027*	10
ANPP _{stem} versus WSI	0.42 ± 0.10	162.9 ± 22.5	0.69	17.9	0.0029***	10

788

789 **Table 2.** Literature values of carbon use efficiencies (CUE) for a broad range of forests

790

Ref.	Vegetation	CUE
This work	<i>Quercus ilex</i> coppice	0.40 (0.37-0.42)
Oechel & Lawrence 1981	MTE spp.	0.38
Waring et al. 1998	Broad range of forests (BRFs)	0.47±0.04
Medlyn & Dewar 1999	BRFs	0.31-0.59
Gracia et al. 1999	<i>Quercus ilex</i> coppice	0.41
De Lucia et al. 2007	BRFs	0.53(0.23-0.83)
Luyssaert et al. 2007	Mediterranean warm evergreen	0.54
Litton & Giardina 2008	BRFs	0.43
Luyssaert et al. 2009	Temp. & boreal forests	0.51±0.02
Piao et al. 2010	BRFs (MAT = 13°C)	0.475
Vica et al. 2012	BRFs with low-nutrient availability	0.42±0.02

791

792 **FIGURES**

793

794 **Fig. 1.** Ordinary least-square regression lines between the water stress integral *WSI* and gross
795 primary productivity *GPP* (light grey circle) and net ecosystem productivity *NEP* (dark grey
796 circle). *WSI* is expressed in MPa day and both *GPP* and *NEP* in $\text{g C m}^{-2} \text{yr}^{-1}$. 2005 data not
797 used in the analysis were also plotted (empty square for *GPP* and empty triangle for *NEP*).

798

799 **Fig. 2.** Ordinary least-square regression lines between the water stress integral *WSI* and the
800 net productivity of stems (dark grey circle and standard-deviation). *WSI* is expressed in MPa
801 day and $ANPP_{stem}$ in $\text{g C m}^{-2} \text{yr}^{-1}$. 2005 data not used in the analysis were also plotted (empty
802 triangle).

803

804 **Fig. 3.** Ordinary least-square regression lines between the water stress integral *WSI* and the
805 net productivity of the reproductive effort (flowers and fruits; dark grey circle and standard-
806 deviation). *WSI* is expressed in MPa day and $ANPP_{reprod}$ in $\text{g C m}^{-2} \text{yr}^{-1}$. 2005 data not used in
807 the analysis were also plotted (empty triangle).

808

809 **Fig. 4.** Ordinary least-square regression lines between the water stress integral *WSI* of the
810 previous year and the aboveground net productivity of leaves of the current year (dark grey
811 circle and standard-deviation). *WSI* is expressed in MPa day and $ANPP_{leaf}$ in $\text{g C m}^{-2} \text{yr}^{-1}$.
812 2005 data not used in the analysis were also plotted (empty triangle).

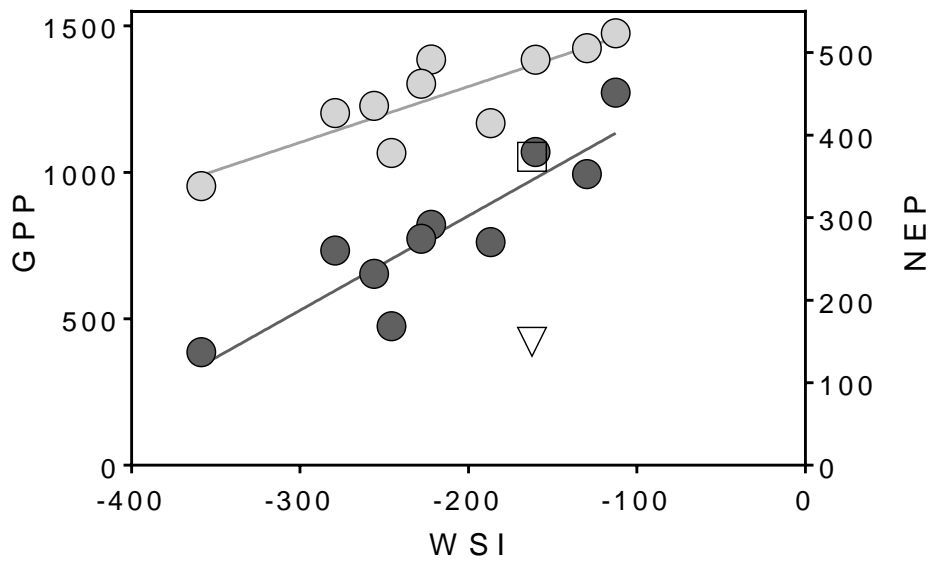
813

814 **Fig. 5.** Change in the partition of gross primary productivity (*GPP*) with increasing drought
815 intensity (*WSI*). The red line displays the decline of *GPP* with decreasing *WSI*. The net
816 primary productivity (*NPP*) components are: perennial aboveground + belowground parts
817 (dark grey), reproductive effort (flowers and fruits; medium grey), leaves and fine roots (light
818 grey). The dashed red curve is for the carbon-use efficiency *CUE*.

819

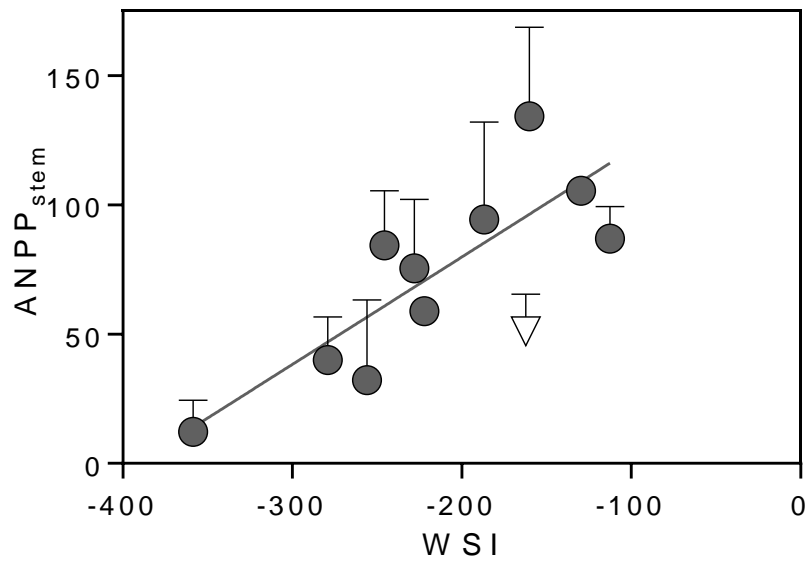
820 **Fig. 6.** Change in the ecosystem respiration, R_{eco} (grey curve), net ecosystem productivity,
821 *NEP* (dark line) and net primary productivity, *NPP* (light grey area) with increasing drought
822 intensity (*WSI*). The dashed red curve is for the R_a/GPP ratio and the brown curve for the
823 R_h/R_{eco} ratio.

824 **Fig. 1.**



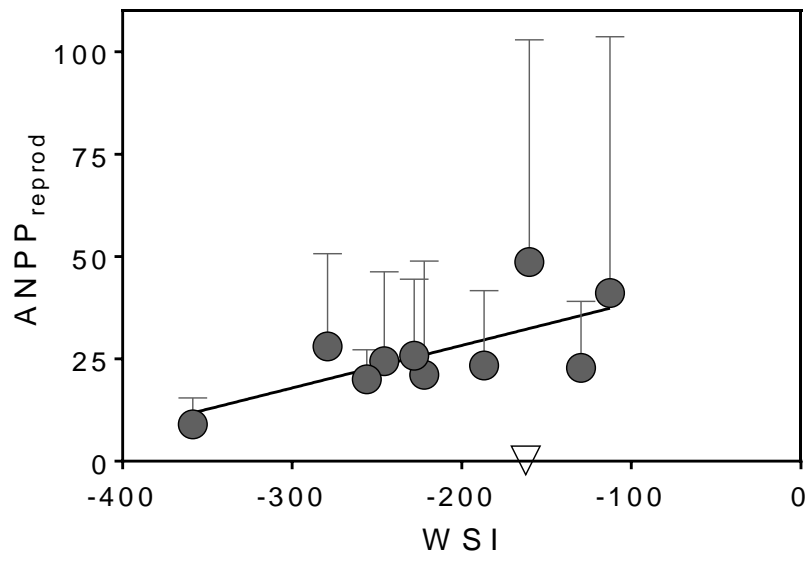
825

826 **Fig. 2.**



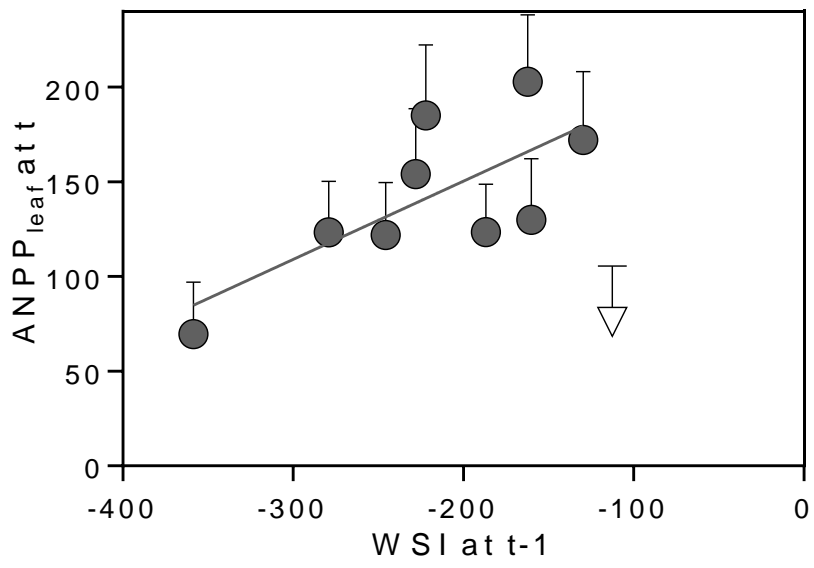
827

828 **Fig. 3.**



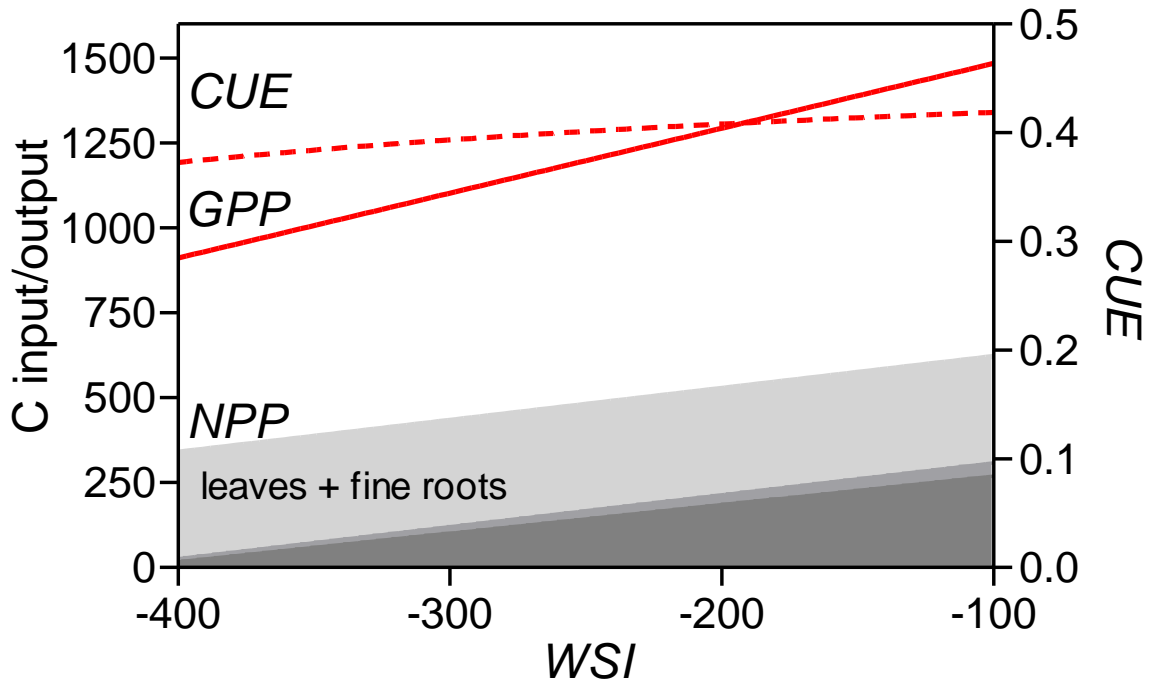
829

830 **Fig. 4.**



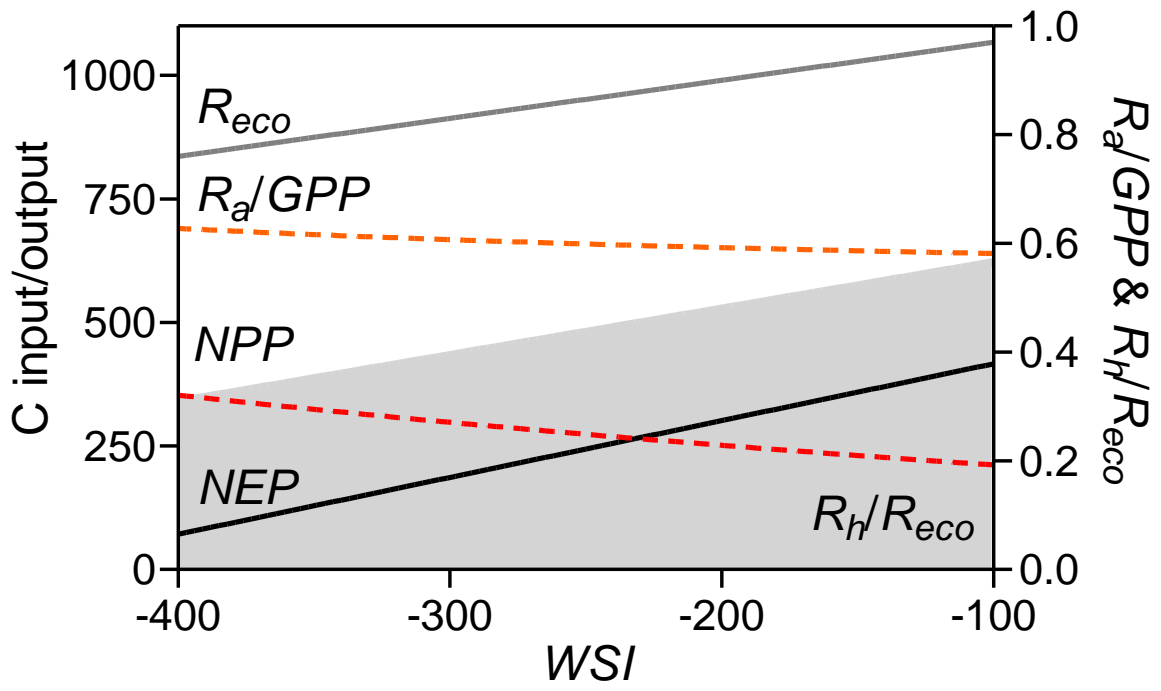
831

832 Fig. 5.



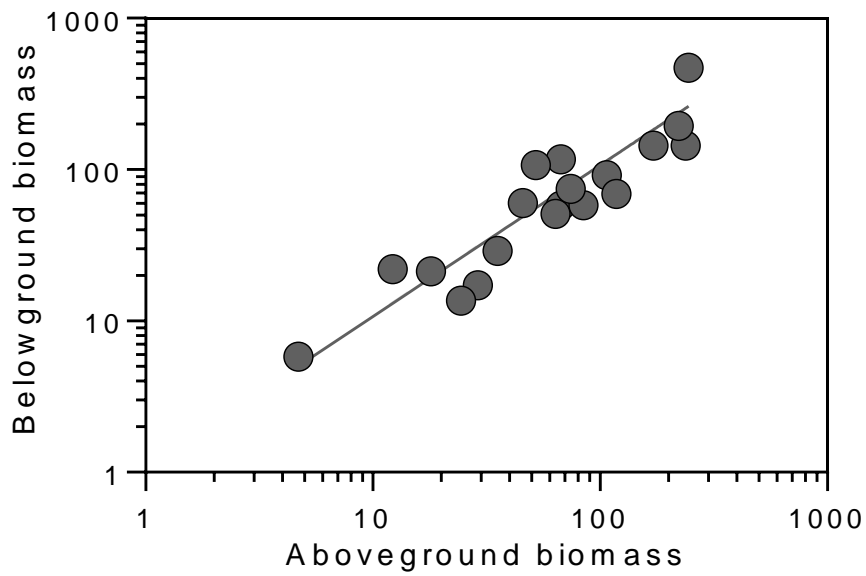
833

834 Fig. 6.

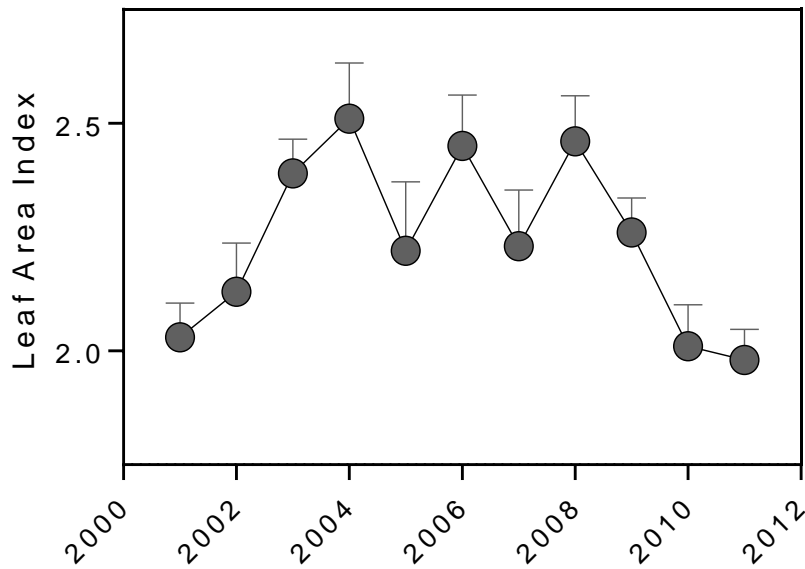


835

Fig. A1. Relationship between aboveground perennial biomass and the corresponding belowground biomass. The belowground biomass is the sum of biomass values for root crown, roots greater than 5 cm, roots ranging from 1 to 5cm diameter.



839 **Fig. A2.** Time course of the peak LAI derived from continuous measurements of half-hourly
840 f_{APAR} between 11 AM and 1 PM from DOY 205 to 225. The Stem Area Index SAI was
841 estimated by image processing of hemispheric photography and assumed constant for the
842 whole period and equal to 0.5. The relationship between leaf area index and water stress
843 integral (WSI) is statistically non-significant.



844